

# Control Strategies for Soft Robot Systems

Jue Wang\* and Alex Chortos

**Soft robots have recently attracted increased attention because their characteristics of low-cost fabrication, durability, and deformability make them uniquely suited for applications in bio-integrated systems. Being fundamentally different from traditional rigid robots, soft robots exhibit properties of infinite degrees of freedom (DOF) and nonlinear materials properties that require innovations in control systems. With the rapid development of materials science, robotics, and artificial intelligence, the diversification of actuator mechanisms and algorithms has enabled a wide range of unique control strategies. This review summarizes the basics of actuator mechanisms and control strategies, including open-loop control, closed-loop control, and autonomous control, and discusses their implementation from diversified perspectives. Control strategies are evaluated based on their compatibility with materials sets, application goals, and implementation route. The emerging directions are forecasted from the perspectives of interfacing between controller and actuator, underactuated control strategies, and implementation of artificial intelligence (AI).**

and polymer composites with stiffness from  $10^4$  to  $10^9$  Pa, which can be easily manufactured manually or by 3D printing and 3D mold technologies at a low cost.<sup>[2,3]</sup> Therefore, there is a low barrier to entry and nearly endless room for creativity.

The strategies required to control soft robots possess major differences compared to those for rigid robots. First, the movement of rigid robots can be specified by the rotation and bending of each joint that is connected by rigid bodies. In contrast, soft robots can deform at all points of the soft materials, resulting in infinite degrees of freedom (DOF), including bending, extension, contraction, and torsion. Second, soft materials exhibit nonlinear and time-dependent materials properties, which make modeling and model-based approaches difficult<sup>[1]</sup> and require further research to establish the internal connection with control science.

In contrast to rigid robots, which typically operate in well-defined environments such as factory assembly lines, soft robots are intended to operate in unstructured scenarios such as assistive robotics<sup>[4,5]</sup> and search and rescue missions.<sup>[6]</sup> This emphasizes the need for soft robots to incorporate sensors that can measure both the state of the environment and the state of the robot itself. In addition, soft robots use diverse actuation mechanisms, such as fluid, heat, electric and magnetic fields, tendons, etc. Different actuation mechanisms require different control systems and sensors. Therefore, the control structure must be designed with knowledge of the actuator mechanisms and sensor properties.

Due to the exciting prospects for soft robotics, many review articles have been published recently covering various aspects of the field. Several reviews longitudinally describe the field, including the aspects of materials, structure, manufacturing, and applications.<sup>[2,7,8]</sup> Such review articles can provide readers with a clear understanding of this enormous field, but have limited space to discuss control strategies. Several reviews focus on subsets of the soft robotics field. Comprehensive reviews on the relationship between materials design and actuation mechanisms for soft actuators have been published by El-Atab et al.,<sup>[9]</sup> Mirvakili et al.,<sup>[10]</sup> McCracken et al.,<sup>[11]</sup> and Chen and Pei.<sup>[12]</sup> Polymerinos et al.<sup>[1]</sup> described many device functionalities in soft robots driven by fluids, including the mechanical properties, strategies to achieve light emission, sensing systems, and a broad description of a number of application spaces, including implantable systems. Laschi et al.<sup>[13]</sup> focus on the large number of abilities that have been developed in soft robots, including growing and self-healing. Thuruthel et al.<sup>[14]</sup> produced a broad survey of control strategies of soft robotic manipulators from

## 1. Introduction

Modern robots originated in the middle of the 20th century. Driven by applications in manufacturing automation, the sophistication of robots has increased exponentially in the past 50 years. During the gradual replacement of the assembly line by robots, the limitations of traditional rigid robots became apparent, such as safety while interacting with humans, resilience to perturbations, and adaptability to various tasks and settings.<sup>[1]</sup> Progress in materials science has enabled breakthroughs toward making robots more similar to biological organisms in both form factors and softness. “Soft robot” is a broad definition that includes mechanical devices with elastically deformable materials and structures that undergo large deformations during operation. Conventional rigid robots are made with high stiffness materials such as steel, which require traditional mechanical machining tools to manufacture. In contrast, soft robots are made of polymers

---

J. Wang, A. Chortos  
Purdue University  
500 Central Dr, West Lafayette, IN 47907, USA  
E-mail: wang5056@purdue.edu

 The ORCID identification number(s) for the author(s) of this article can be found under <https://doi.org/10.1002/aisy.202100165>.

© 2022 The Authors. Advanced Intelligent Systems published by Wiley-VCH GmbH. This is an open access article under the terms of the Creative Commons Attribution License, which permits use, distribution and reproduction in any medium, provided the original work is properly cited.

DOI: [10.1002/aisy.202100165](https://doi.org/10.1002/aisy.202100165)

the perspective of control science and algorithms. This review provides a survey of interdisciplinary topics that contribute to the development of control strategies, including materials and actuation mechanisms and bio-inspired concepts.

To introduce the control strategies of soft robots for broad audiences, we start from actuator mechanisms that are activated by different energy sources. In the section “Control Strategies,” open-loop, closed-loop, and autonomous control of soft robots are reviewed based on the traditional scope of control science, but a biological explanation of such types of control is proposed as a metaphor for the bionic principle of soft robots. The section “Control Implementation” discusses the details of the strategies for implementing control structures with different types of actuators. A key trend in the field is to create lightweight and miniaturized devices. As the number of actuators and controllable DOF increase to meet complex applications, it is important to develop efficient control strategies that minimize the volume and power requirements of the control system, especially for autonomous or energy-constrained systems such as wearable devices or swarm robots. Thus, in the section “Emerging Directions,” we discuss new approaches to interface between the control system and actuators.

## 2. Actuator Mechanisms

In this section, we review actuator mechanisms according to the source of energy that drives them, which determines the nature of the control system. The specific classifications are fluidic-driven, electric-driven, and magnetic-driven. Stimulus-driven actuator mechanisms, such as pH and humidity, typically do not have a control system and will therefore not be discussed in detail.

### 2.1. Fluidic-Driven Actuator Mechanisms

Actuation driven by the pressure of gas or liquid inside a deformable bladder is the most widely used actuation mechanism due to their relative ease of fabrication. Hydraulic systems possess high power density, which can be used in applications that require large force and torque.<sup>[15]</sup> In addition, hydraulic systems have unique advantages in underwater applications due to compatibility with the environment.<sup>[16]</sup> Pneumatic actuators exhibit lower power and more complex control due to the compressibility of the gas (Figure 1i).<sup>[17]</sup> For miniaturized devices, pneumatic actuators are advantageous because their valves and sources can be more easily miniaturized and air acts as an omnipresent gas source. In addition, pneumatic actuators have a low barrier to entry due to widely available commercial microcontrollers and pneumatic hardware from companies such as FESTO, SMC, and Parker.

A variation of pneumatic actuators relies on the jamming of granular media to change the stiffness of a component (Figure 2j).<sup>[18–21]</sup> Jamming-based grippers<sup>[18,19]</sup> have the advantage that they can pick up a wide range of objects without the need for active feedback. Meanwhile, the stiffness tuning characteristic of jamming-based actuators can be used in the linkages of continuum soft robots.<sup>[20,21]</sup> Most fluidic-driven actuators are made of soft elastomers, which results in low radial stiffness.

Introducing origami structures composed of stiff materials can improve the stiffness and carrying capacity of the pneumatic robot while retaining the compliant characteristics.<sup>[22–24]</sup> By modifying the shape, volume, and stiffness-tunable characteristics of origami structures, a soft robot with multiple tunable features can be achieved.<sup>[25]</sup>

Traditionally, tethered fluidic actuators have been powered by conventional pumps. For untethered applications, onboard compressed fluid cylinders and microcompressors have been implemented. However, these energy sources require electrical control hardware. To reduce system complexity, generating gas pressure through chemical reaction<sup>[26,27]</sup> has been implemented using two methods. The first is the explosive combustion realized by methane ( $\text{CH}_4$ ) and butane ( $\text{C}_4\text{H}_{10}$ ). The combustion of these two substances possesses high energy density and high reaction speed, but it requires a fuel source, oxygen source, and ignition source. The second method does not require an ignition source, and is based on the decomposition of peroxide monopropellant such as hydrogen peroxide. The conversion rate of hydrogen peroxide into gas can be increased by adding a catalyst.<sup>[28–30]</sup> As the generated heat is much lower compared with explosive combustion, safety concerns are reduced.<sup>[31]</sup>

### 2.2. Electric-Driven Actuator Mechanisms

Electrical energy can be converted to the deformation of soft materials using two general approaches: direct conversion of electric fields to mechanical deformation, and indirect conversion through another form of energy (mechanical, thermal, or optical). While the indirect approach uses different mechanisms for actuation, such as thermal expansion or phase changes, we classify it as indirect electrical actuation from the perspective of the stimulus that is used to control the actuation. Other reviews give detailed descriptions of the mechanisms.<sup>[9–12]</sup>

The “direct way” of addressing obtains force directly from the electrostatic field. The mechanism of how the electric field is converted into mechanical deformation depends on the properties of the material. Dielectric elastomer actuators (DEAs) use the attractive force between positive and negative charges on opposite electrodes to deform a soft elastomer dielectric (Figure 1b).<sup>[32–37]</sup> DEAs can be prepared from low-cost materials using manual<sup>[38]</sup> or automated fabrication approaches<sup>[39–42]</sup> and possess advantages of large strains and fast actuation speeds.

Piezoelectric materials contain aligned dipoles that either change in magnitude or spacing in the presence of an electric field (Figure 1a).<sup>[43–45]</sup> Piezoelectric materials actuate within the elastic range of high-modulus materials, enabling high stresses, fast actuation, and minimal mechanical dissipation. Their key drawback is low actuation strains.<sup>[43]</sup> While most piezoelectric materials are not considered soft, they can be incorporated into soft form factors through geometric patterning.<sup>[44,45]</sup> Ionic electro-active polymer actuators (IEAPAs) rely on the movement of ions in an electrolytic capacitor in response to an electric field. This ionic polarization provides large bending displacement at low voltages<sup>[46–49]</sup> with limitations of low force output and the requirement of encapsulation to operate in ambient conditions.<sup>[50]</sup> Hydrogels respond to electric fields based on a similar mechanism as IEAPAs, but can also be stimulated by humidity,

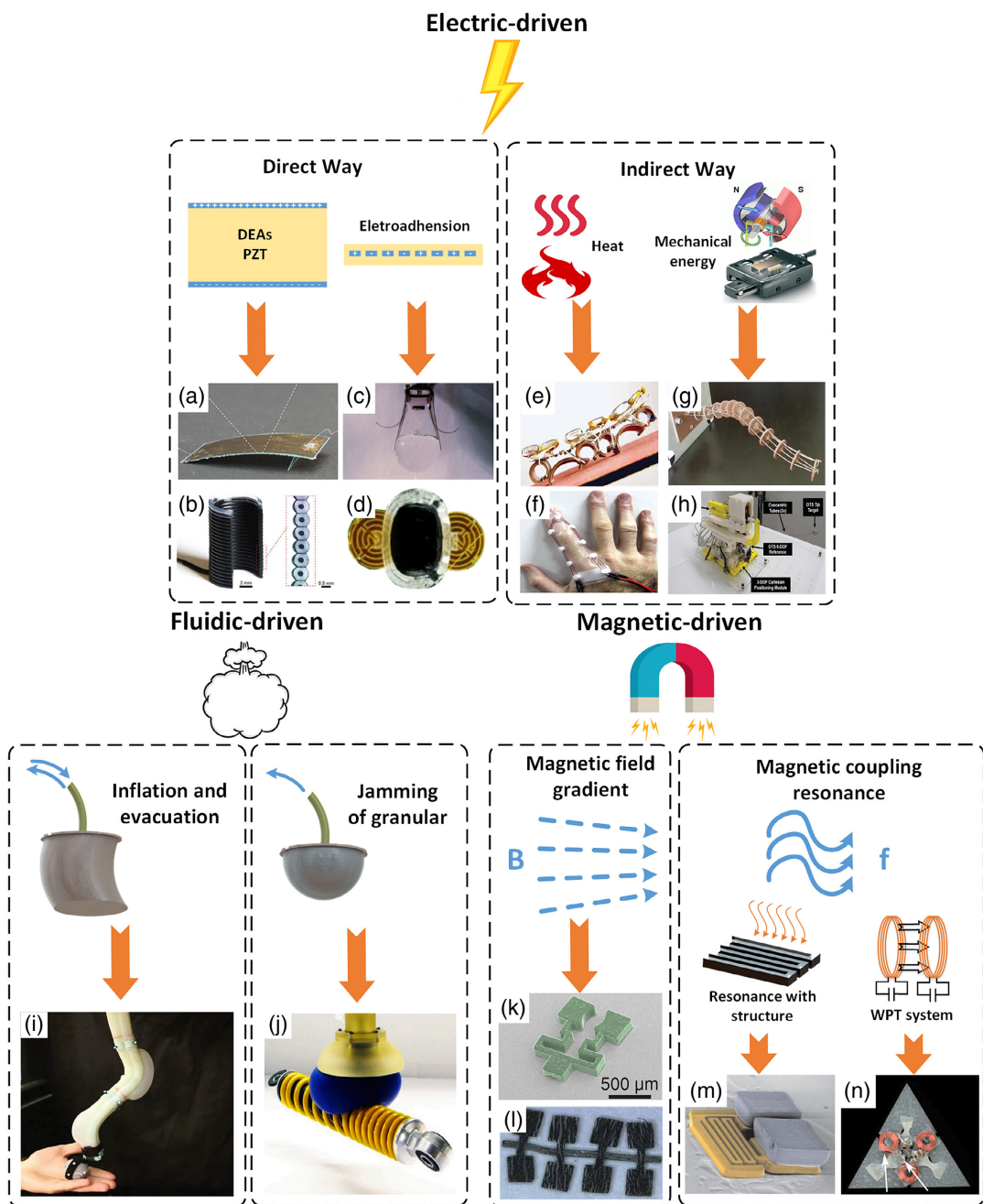


**Figure 1.** Diversity of actuator mechanisms in soft robots. a) Curved unimorph piezoelectric actuator. Reproduced with permission.<sup>[218]</sup> Copyright 2019, AAAS. b) Dielectric elastomer fiber actuator. Reproduced with permission.<sup>[32]</sup> Copyright 2021, Wiley. c) Soft gripper based on electroadhension. Reproduced with permission.<sup>[57]</sup> Copyright 2016, Wiley. d) Soft wall-climbing robot based on electroadhension. Reproduced with permission.<sup>[58]</sup> Copyright 2018, AAAS. e) Highly dynamic SMA actuator. Reproduced with permission.<sup>[64]</sup> Copyright 2018, AAAS. f) Soft wearable device using TCP actuators. Reproduced with permission.<sup>[69]</sup> Copyright 2019, IEEE. g) Tendon-driven soft continuum robot actuated by an electromagnetic motor. Reproduced with permission.<sup>[350]</sup> Copyright 2019, SAGE. h) Tendon-driven soft continuum robot actuated by a piezoelectric motor. Reproduced with permission.<sup>[63]</sup> Copyright 2012, IEEE. i) Pneumatic soft continuum robot. Reproduced with permission.<sup>[17]</sup> Copyright 2016, SAGE. j) Gripper based on the jamming of granular. Reproduced with permission.<sup>[18]</sup> Copyright 2010, PNAS. k) Untethered micro-grippers driven by magnetic field gradient. Reproduced with permission.<sup>[87]</sup> Copyright 2014, Wiley. l) Millimeter-scale flexible robot driven by magnetic field gradient. Reproduced with permission.<sup>[214]</sup> Copyright 2019, AAAS. m) Untethered microrobot driven by magnetic coupling resonance. Reproduced with permission.<sup>[94]</sup> Copyright 2010, SAGE. n) Folding robot driven by wireless power transfer system based on magnetic coupling resonance. Reproduced with permission.<sup>[104]</sup> Copyright 2017, AAAS.

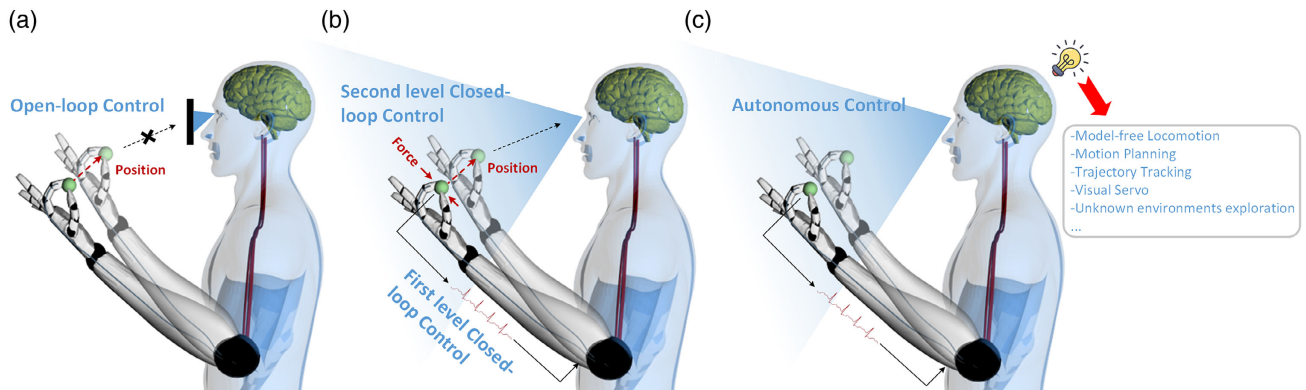


**Figure 2.** The biological explanation of soft robot control strategies. a) Open-loop control. b) Closed-loop control (First-level closed-loop control and second level closed-loop control). c) Autonomous control.

temperature, pH, and light.<sup>[51]</sup> This indicates that it can be self-powered under multiple fields and the synergy of multiple controllable sources could provide multidimensional control.<sup>[52]</sup>

In addition to stimulating actuation, electric fields can be used to modify materials properties or device adhesion. Colloidal-like electrorheological fluids (ERFs)<sup>[53–55]</sup> consist of a carrier oil with microparticles that aggregate in response to an electric field, causing the material to dramatically change in stiffness. ERFs can be used for control valves for fluid-driven soft robots<sup>[53]</sup> or to tune the rigidity of fluidic artificial muscles.<sup>[56]</sup> The electrostatic effect of constriction between two surfaces subjected to an electrical field, which is called electroadhesion, is also widely used in soft robots.<sup>[57–60]</sup> (Figure 1c,d) From the perspective of electrodes' structure, flexible electroadhesive devices (EA) can be divided into two strategies. The first is to generate electric fields between alternating electrodes that attract free charges in conductors and cause polarization in insulating substrates. This strategy is popular in grippers<sup>[57,59]</sup> and climbing robots.<sup>[58]</sup> The second strategy uses planar electrodes between a device and substrate, which is widely applied for clutches.<sup>[60]</sup> The principle of electroadhesion can also be classified into two categories depending on whether the adhesion object is a conductive or insulating substrate.<sup>[61]</sup>

The actuation mechanisms of “direct way” possess advantages of high electromechanical conversion efficiencies and simple device structures. However, the direct electromechanical conversion mechanisms each have a drawback, including low actuation stress for DEAs and low actuation strain for piezoelectrics. In addition, DEAs and piezoelectric actuators require high-voltage sources and control systems. Transferring the electrical energy to another form (indirect way) can support many other actuation mechanisms with different characteristics. Electrical energy can be converted to mechanical energy at one location and then transferred to another location, allowing the use of non-soft actuators in soft systems. For example, mechanical energy generated by electromagnetic<sup>[62]</sup> and piezoelectric<sup>[63]</sup> motors can deform soft robots using tendons. A widely implemented indirect conversion consists of transferring electrical energy to heat using Joule heating, which can be used to drive phase transformations in shape memory alloys (SMAs)<sup>[64,65]</sup> (Figure 1e).

Liquid crystal elastomers (LCEs) provide fully reversible thermally activated phase changes that can achieve 60% contractile strains.<sup>[66]</sup> These electrothermally induced phase transformations provide very large actuation stresses. Similarly, thermal energy can be converted into deformation using differences in thermal expansion coefficients between materials.<sup>[67,68]</sup> Twisted and coiled polymer (TCP)<sup>[69,70]</sup> configurations can convert these thermal expansion mismatches into large tensile displacements (Figure 1f).

While Joule heating directly converts electrical energy into heat, converting electrical energy into light provides a mechanism to activate materials remotely. The simplest light-based strategy is to generate thermal energy in a material through the absorption of light, referred to as photothermal heating. This allows remote activation of thermally activated mechanisms including thermal expansion<sup>[71]</sup> and phase-change materials such as LCEs.<sup>[72]</sup> Alternatively, materials have been engineered that change their polymer conformations when exposed to light. For example, the light-induced change in the conformation of azobenzene moieties can increase the volume of a material, enabling light-mediated bending actuators.<sup>[73,74]</sup> Light-based stimulation provides a high-resolution approach that is viable when a large external control system can be used.

An important drawback of the indirect electrical way of addressing soft actuators is that each step of energy conversion leads to energetic losses. For example, for photothermal actuators, electricity is supplied to the optical device (light-emitting diode (LED) or laser) and some of that electrical energy is converted into optical energy. Subsequently, some of the optical energy is converted into thermal energy in the actuator.<sup>[75]</sup> Consequently, these types of actuators have low efficiencies that hinder their implementation in untethered systems. They are often used when the energy source and control system can be powered externally, such as optical control of microrobots.<sup>[76,77]</sup>

### 2.3. Magnetic-Driven Actuator Mechanisms

Magnetically driven soft robots have grown in popularity due to the potential to generate large actuation forces using remotely generated magnetic fields. Similar to the electric-driven actuator

mechanisms, magnetic counterparts can also be divided into two categories based on direct and indirect activation.

The direct way of addressing can be distinguished by the type of material. Ferromagnetic materials retain a permanent magnetic dipole. Magnetic field gradients can interact with these magnetic dipoles to produce local directional forces on materials elements (Figure 1k,l) Paramagnetic materials form a dipole only when a magnetic field is present. When paramagnetic particles are incorporated into a composite material, the application of a magnetic field causes the particles to attract each other through dipole–dipole interactions, inducing changes in the stiffness (magnetorheology)<sup>[78]</sup> or shape (magnetostriction).<sup>[79]</sup> Magnetorheological materials perform similar roles as electro-rheological materials in tuning the stiffness of elements of soft robots, but with the key difference, that magnetic fields can be remotely generated.<sup>[78]</sup> For both ferromagnetic and paramagnetic materials, the principle of the force and torque generated in a magnetic field can be described by the following formula

$$\mathbf{F} = \nabla(\mathbf{m} \cdot \mathbf{B}) \quad (1)$$

$$\mathbf{T} = \mathbf{m} \times \mathbf{B} \quad (2)$$

where  $\mathbf{m} = q_m \mathbf{d}$  is the magnetic dipole moment due to two equal and opposite magnetic charges  $q_m$  that are separated by a distance,  $d$ , which comes from the concept of electric dipole moment  $p$  due to electrical charges, and  $\mathbf{B}$  is the magnetic flux density.

For simple control applications, microrobots can be driven manually by moving permanent magnets relative to the soft robot.<sup>[80–83]</sup> Fabricating robots with tailored magnetic dipole orientations in each pixel can achieve sophisticated deformations in response to a magnetic field. This approach has been enabled by recent innovations in patterning ferromagnetic elements in complex 2D and 3D layouts, including direct ink write (DIW) printing,<sup>[84]</sup> local lithographic patterning,<sup>[85]</sup> and photothermal patterning.<sup>[86]</sup> However, if complicated and controllable multi-DOF motion is required, a coil system is needed to achieve accurate spatial and temporal control of the magnetic fields using coil systems.<sup>[81,87–93]</sup> The details will be introduced briefly in Section 4.1.

Magnetic actuators that mechanically oscillate at specific frequencies of AC magnetic fields can provide selective control and achieve improved energy density in microrobots (Figure 1m).<sup>[94–96]</sup> Compared with DC magnetic fields, this oscillating spring–mass approach allows microrobots with larger actuation magnitude since the resonance effect can increase the energy transfer efficiency.

As to the indirect way, magnetic materials can be used to convert the energy of a magnetic field into a different form. For example, based on the Néel and Brownian relaxation process of ferromagnetic nanoparticles, the energy in a magnetic field can be transferred to heat, enabling a thermal bending actuator.<sup>[97]</sup> Magnetic shape-memory alloys (MSMAs) are another material that can absorb energy from magnetic fields. MSMA actuators (made by Ni–Mn–Ga, Fe–Pd, and Ni–Mn–Al) possess advantages of high stiffness and low-temperature operation, but provide low actuation stress and are difficult to shape.<sup>[98]</sup> To increase the controllable parameters of the control system, an AC magnetic field for heating the materials can be combined

with a DC magnetic field for dragging the robot to create more complicated motions.<sup>[97,99]</sup>

Transferring energy using the magnetic properties of materials is typically limited by low power density. After mid-range power transfer based on strong magnetic coupling resonance (MCR) was developed in 2007,<sup>[100]</sup> magnetic energy can be transmitted efficiently over long distances.<sup>[101]</sup> In such wireless power transfer (WPT) systems, an antenna LC coil generates an oscillating electromagnetic field. Receivers consist of LC coils that are tuned to oscillate within a narrow frequency range and convert electrical oscillations into DC power for an actuator using a rectifier. By creating multiple LC resonators with different natural frequencies, one control antenna can selectively activate multiple actuators by changing the frequency components in the electromagnetic control signal.<sup>[102]</sup> Such multiplexing features will be discussed in Section 5.2. In addition, the magnitude of the energy absorbed by the receiver coil is related to the distance between the antenna coil and the receiver, providing a mechanism for self-sensing feedback. In fact, even though it is based on the magnetic source, the receiver converts the magnetic energy into electrical energy that can be used in diverse actuator mechanisms. Transferring magnetic energy to thermal energy is a promising way to drive phase-changing actuator mechanisms. For example, magnetic heating of SMAs has recently led to demonstrations of a continuum robotic caterpillar<sup>[103]</sup> and an origami gripper with a bending function.<sup>[104]</sup> Similarly, energy from a WPT system was converted to thermal energy that converted a liquid to gas, activating a fluidic actuator.<sup>[105]</sup>

### 3. Control Strategies

In this section, control systems are divided into three strategies, including open-loop, closed-loop, and autonomous control. We introduce each classification using a biological analogy.

#### 3.1. Open-Loop Control

Open-loop control involves predicting movement based on knowledge of the robot and the space in which it is operating. For example, to move a tennis ball to a desired location without tactile or visual feedback (Figure 2a)), muscle memory and experience must be used. However, after establishing a precise model which resembles the muscle memory and experience modeled in human being's brain, accurate motion of soft robots can be achieved without sensors for feedback. As shown in Figure 3a), the control diagram of open-loop control transfers the reference input of the system ( $r$ ) to the controller input ( $u^*$ ) through the mathematical model of the actuator. Then the role of the controller is to adjust  $u^*$  to the input ( $u$ ) for the actuator. Finally, the  $u$  will turn to the current status of the actuator,  $y$ , inversely by the actuator whose physical characteristics have been predicted in the model. In a broad sense, any control without feedback can be considered as an open-loop. Thus, the non-model on/off switch control, which is especially popular in soft robotics, can also be seen as an open-loop control strategy. Although a single actuator with on/off control typically employs a simple control algorithm, a system with several on/off

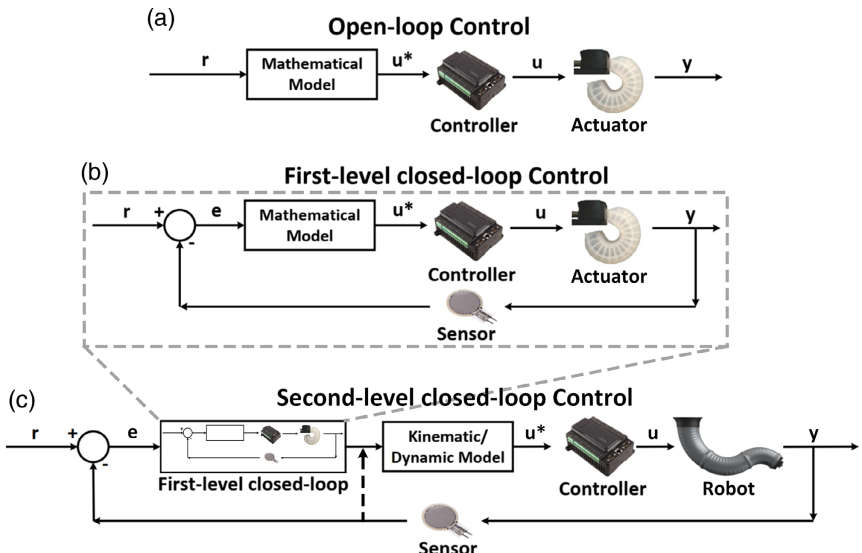


**Figure 3.** Diagram of different kinds of control. a) Open-loop control diagram. b) First-level closed-loop control diagram. c) Second-level closed-loop control diagram.

actuators requires an advanced control algorithm to coordinate between actuators to accomplish locomotion.<sup>[106]</sup>

Finite element method (FEM) discretizes a system into elements and iteratively calculates the state of the system using defined mathematical relationships between the nodes of the elements. It is the most general method of open-loop modeling because it can be applied to any shape or actuation mechanism. Since commercial FEM software (e.g., ANSYS, ABAQUS, and COMSOL) are computationally expensive, FEM is typically used for offline validation of the analytical models and experimental results<sup>[107,108]</sup> or offline prediction of the actuators' movement.<sup>[109]</sup> Therefore, it has mostly been implemented for open-loop control of soft robots since it is difficult to include feedback in real time. Many commercial FEM software provide multi-physics packages that can reduce the barrier to entry.

Analytical models based on physics or mathematics<sup>[22,23,107,110]</sup> make assumptions based on the structure of the robot to reduce the number of DOFs. This reduces the computational burden compared to FEM. Kinematics models derive the quasistatic deformation of the robot. They express a relationship between actuator input and robot deformation. Forward control can then be achieved by defining the actuator inputs in the model and calculating the resulting robot displacements. Inverse control is achieved by defining the desired robot displacements and using the model to calculate the necessary actuator inputs. Dynamic models predict the time-dependent changes in the robot structure, enabling control of the velocity and acceleration in semi-soft<sup>[111–114]</sup> or fully soft continuum robots.<sup>[115–117]</sup> Although analytical models have very good computational efficiency, they are typically specific to a particular form of robot and make assumptions about the robot structure and actuation mechanism that limit the accuracy. Analytical models can only be developed by someone who has a strong background in the physics of the actuator mechanism and robot structure.

Model-based open-loop control strategies all start with the structure design and then develop a model to predict the motion of the specific structure. However, in practical applications, the robot structure is designed to achieve a target motion. Thus, one of the key challenges in this field is to solve this inverse problem: how to design the robot structure to achieve a specified motion or function. The key limitation of open-loop control is that there is no feedback mechanism to indicate when the actuator reaches the desired state. Open-loop control is, therefore, limited to situations in which the environment and properties of the objects that the robot will interact with are already well known.<sup>[1]</sup> Environmental conditions that may change include encountering unexpected obstacles or changing global variables such as temperature that might affect the materials' properties of the robot. The properties of the robot that can be difficult to model include manufacturing defects and difficulty in considering materials with complex or time-varying properties. Small non-idealities in taking time-varying materials properties into account can propagate through sequential actuation tasks to result in large errors when no feedback is present.<sup>[38,103]</sup> As a result, open-loop control is typically used for short or repetitive tasks.

### 3.2. Closed-Loop Control

Closed-loop control relies on sensors to provide feedback about the deformation state of the actuators and their contact state with the surrounding environment. Closed-loop control is necessary when the environment or task is varied or uncertain, such as an untethered robot that will traverse uncertain terrain or a gripper that will pick up different sizes and shapes of objects. The diverse actuation mechanisms and wide range of physical structures for soft robots enable and require the implementation of a large variety of sensing strategies.

From the perspective of biology, biological systems possess two mechanisms of closed-loop control. The first is

proprioceptive sensors in the form of strain-sensing neurons that are built into the muscles and joints. As shown in Figure 2b), the feedback signals from strain-sensing neurons facilitate grasping a tennis ball with the desired force. Here, only the internal “sensors” are integrated into the actuator mechanisms (the arm). The second is visual feedback, which is often necessary for achieving very precise movements such as serving a tennis ball. The external visual feedback can facilitate the movements of the arm using closed-loop control.

In the field of robotics, closed-loop control can be divided into two levels like the biological systems mentioned earlier. The first level is the feedback that controls the deformation state of individual actuators.<sup>[118–121]</sup> Here, in the joint space, as shown in Figure 4, the input is the actuator stimulus, such as pressure, voltage, temperature, etc., and the output is the geometric parameters of actuator, such as angle, length, etc. In other words, the control of joint space ensures a particular deformation state of the joint but does not take into account the deformation state of the overall robot, so kinematics is not required. Such control strategies are common for soft robots that have one actuator. For multi-actuator robots, totally decoupled systems such as a soft gripper with individual actuators can achieve target operation by joint space control without considering the connections between each actuator.<sup>[122]</sup> As depicted in Figure 3b), the forward route is the same as open-loop control, but the sensor integrated on the actuator will add feedback to the reference input of the actuator ( $r$ ) before it is brought into the model.

The second-level control is located on the configuration space and task space. The inputs into the second-level controller are the geometric parameters of the actuators (output of first-level control) and the output of the second-level controller is the geometric parameters of the entire robot body. The second level controller includes the kinematics and dynamics of the robot body.<sup>[123–126]</sup> The configuration space includes all possible poses of the robot body that can be formed given the range and limitation of each individual joint. As illustrated in Figure 4, the robot control in the configuration space takes into account the configuration of each joint to obtain the position of the end-effector. Forward kinematics is used to map the joint space to the configuration space and inverse kinematics do the opposite. The task space only considers the position, orientation, or force of the end-effector. Since they are determined when the configuration of each joint is specified, the task space can be considered as a subset of the configuration space which has fewer parameters.

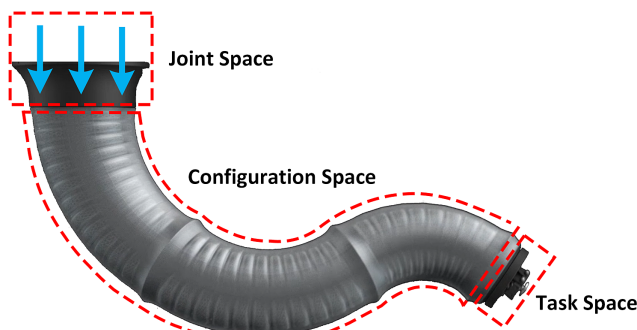


Figure 4. Definition of three different spaces.

Most of the task space control examples are inverse tasks, which means such control problems start from the desired position of the robot and work backward to determine the necessary actuation state of each joint. Thus, inverse kinematics/dynamics play a significant role in the space control problem. One of the important application opportunities for soft robots is in the autonomous exploration of unstructured environments. In this situation, there is no obvious distinction between the configuration space and task space when the robot does not have a fixed reference point.

The diagram of second-level closed-loop control is shown in Figure 3c), which can be considered as an outer loop over the first-level closed-loop. Here, the reference input  $r$  still inputs to the joint space located in the first-level closed-loop. Then, the output of the first-level closed-loop becomes the input of the second level. The controller in the second level is the mathematical model of the kinematics and dynamics. The sensor's feedback of the second-level loop, the entire robot body, can be added before and after the first-level closed-loop. The sensors added before the first-level closed-loop are usually located on the joint space whose roles are to detect the physical parameters of actuators (pressure, voltage, etc.). While the sensors detecting the displacement or configuration error of the end-effector should provide feedback to the signals after the processing of the first-level closed-loop.

After classifying the closed-loop control in the robotic perspective, the first-level closed-loop can be further classified according to the sensor types. The first category is the detection of indirect variables of actuator mechanisms, such as internal pressure for fluid-driven mechanisms<sup>[119,127,128]</sup> and current and voltage for electric-driven mechanisms (self-sensing feedback).<sup>[129–132]</sup> These internal variables reflect the input value to the actuator (e.g., pressure or voltage). The sensors for internal variables are usually integrated into the actuator mechanisms. A model must be used to estimate the deformation state of the actuator based on the internal variable.

Variables such as strain,<sup>[133]</sup> angle,<sup>[134]</sup> and contact force<sup>[135]</sup> are called external variables. They provide direct information about the deformation state of the system. However, because the sensors for these variables should be mounted on the robot structure, closed-loop control in soft robots is enabled by the development of soft sensors and fabrication methods that integrate sensors and actuators.<sup>[133]</sup>

Second-level closed-loop control strategies can be further classified based on the type of model (static vs. dynamic) and the space on which the controllers act. The most common approach is to use a static kinematic model in the configuration/task space with a joint space controller because it possesses a faster and more stable response. Dynamic models typically locate their controller in the joint space since dynamic models directly map the variables in the joint space to the task space.<sup>[14]</sup>

Although closed-loop control can be seen as a step forward from open-loop control, there are still some limitations of closed-loop control. First, since closed-loop control strategies are model based, their universality is limited because one model can be only applied to a particular soft robot system. Second, miniaturization is one of the key development trends in soft robots. As devices are miniaturized, the materials and manufacturing processes for making small sensors integrated

with actuators become a limiting factor. Consequently, most untethered soft robots with large numbers of actuators,<sup>[136]</sup> or very small sizes<sup>[137]</sup> use the simplest open-loop switch control instead of using closed-loop control. In contrast, developing onboard control systems with flexible and integrated microsensors arouse great interest in recent years.<sup>[138]</sup>

Since one potential application of soft robots is to integrate with human beings or other organisms, another challenge is to receive signals from biological systems that can be integrated into the control of the soft robot. These signals can come from flexible sensors or organisms, such as electrooculography (EOG), electroencephalography (EEG), and electromyogram (EMG) signals.<sup>[124]</sup> Quantifying and processing these biological signals will enable bio-hybrid soft robots with human control.

### 3.3. Autonomous Control

In the field of soft robotics, “autonomous” is often used to describe systems that can operate without input from an external power source or control system, which can also be called onboard control.<sup>[139,140]</sup> We want to distinguish this from the concept of autonomous control systems: the controller that has its own “brain” to adapt, predict, and learn the parameters, architectures, and models of control. To this extent, autonomous control can be seen as an enhancement to the previously described control strategies. All the control diagrams shown in Figure 3 can be transferred to autonomous control. The core difference is that the algorithms in the “Model” box and the parameters in the “Controller” box can be generated automatically using analytical optimization methods<sup>[141]</sup> or machine learning (ML).<sup>[142]</sup> Under the perspective of biology shown in Figure 2c), taking the same example of serving a tennis ball, you can move the ball to an accurate position only by visual feedback. But what angle or height do you need to throw the ball from based on the wind, your height, your arm length, or your batting habits? These controls require the participation of your brain, which means that you need to use your brain's long-term learning experience to complete them. Under these circumstances, pure closed-loop control cannot meet the requirements. The addition of learning tools makes the control become “autonomous” or “intelligent”.

Achieving a specific task using open-loop control can be enabled by designing the structure of a robot appropriately. This inverse process of designing a robot to accomplish target movements can be enabled by automated design processes.<sup>[141]</sup>

In the joint space, ML algorithms can be used to identify the parameters of physical models of soft actuators<sup>[143]</sup> and sensors.<sup>[144,145]</sup> Then, these physical models can be used to establish relative adaptive control.<sup>[120]</sup> In the configuration and task space, obtaining kinematic or dynamic models of the entire robot system<sup>[146–148]</sup> through ML algorithms can be considered as an offline autonomous control strategy. Online autonomous control strategies can be classified into model-based control including adaptive<sup>[149,150]</sup> and predictive control<sup>[151,152]</sup> and model-free control implemented with ML algorithms.<sup>[142,153,154]</sup> These autonomous control strategies have achieved trajectory tracking,<sup>[155]</sup> vision-servo,<sup>[156]</sup> motion planning,<sup>[157]</sup> and exploration and adaptation of unknown environments<sup>[158]</sup> such as random force and complex terrains.

Just like the FEM-based open-loop control, ML algorithms are limited by high computational costs. Therefore, one of the key challenges in the field is to reduce the computational complexity of ML algorithms as well as improving the accuracy of the algorithm. Typically, for soft robots, one of the critical limitations in ML is that the prediction is only as good as the data set. Training a robot to function in unfamiliar terrain is not straightforward. Additionally, the use of ML algorithms makes it difficult to understand the fundamentals of how the robot design affects its function because ML algorithms act as a “black box” between the robot and the control.

## 4. Control Implementation

The approaches used to implement different control strategies vary based on the actuator mechanism. In this section, the implementation of different control strategies to different actuator mechanisms will be introduced based on the classification of control strategies.

### 4.1. Open-Loop Control

FEM is one of the most popular open-loop control strategies. Soft actuators enable continuous deformation throughout all points of the material, while FEM is based on representing the robot as discrete elements. A key step in developing an appropriate FEM model is to choose the size of elements that is small enough to accurately approximate the continuous deformation of the system without excessively increasing the computational time of the simulation.<sup>[159]</sup> Although FEM is widely used to model all actuator mechanisms, there are many differences in implementation principle and simulation conditions. A key step in increasing the accuracy of FEM models is to incorporate the relevant physics of the system into the equations governing the behavior of each node. For example, when simulating an elastomer material in commercial software such as ABAQUS, COMSOL, or AYSYS, either a built-in hyperelastic model or user-defined stress-strain model can be used to create a quasistatic model. Simulating the dynamic behavior of the deformation requires implementing the equations for the viscoelastic properties.<sup>[160]</sup> For fluidic-driven actuators, models only need to consider solid mechanics. The action of the fluid stimulation is modeled with boundary conditions. Similarly, for tendon-driven soft robots,<sup>[161,162]</sup> the electromagnetic and piezoelectric motor drive the soft robots indirectly. Here, only the interaction between tendon and robot structure needs to be considered, which has a similar implementation as fluidic-driven soft robots.

Specifying the governing equations for electromechanical actuators<sup>[35]</sup> requires including the effect of the electric field in the FEM simulations. ABAQUS achieves this coupling using a UMAT subroutine<sup>[160,163–165]</sup> while it can be defined as a multi-physics field in COMSOL.<sup>[166–168]</sup> Increasingly accurate models for DEAs are being developed by including the effects of material viscoelasticity and the rate of heat generation due to viscoelastic dissipation.<sup>[169]</sup> Including the effect of electrode resistance could improve simulations of the dynamics of DEAs.<sup>[170]</sup> IEAPAs are simulated by using the Nernst–Planck equation to determine the ionic concentration caused by the applied potential difference

and then deriving the strain through the relationship between force and ionic concentration. Thermally driven actuators, such as SMA<sup>[171,172]</sup> and TCP,<sup>[173]</sup> require the incorporation of thermal effects in simulations. In magnetic-driven actuator mechanisms, magneto-mechanical coupling equations express the relationship between the applied field and the generated force, while solid mechanics determines the relationship between the torque and deformation.<sup>[174–177]</sup> For example, simulating electromagnetic actuators<sup>[177]</sup> in COMSOL requires “Magnetic Fields,” “Magnetic Fields, No Currents,” and “Solid Mechanics” multi-physics fields to simulate the coils, permanent magnets, and soft materials, respectively.

Due to high computational time, FEM has often been used for validation or prediction. FEM has been used in the inverse design of robot structures by prescribing the amount of actuation necessary to reach a goal in a multi-actuator robot.<sup>[161,162]</sup> Reducing the computational burden of FEM so that it can provide control information during real-time deformation of the robot extends the utility of FEM to closed-loop control. By making simplifying assumptions such as using linear elasticity and a coarse mesh (1000 nodes), Duriez et al. achieved a refresh rate of 60 Hz.<sup>[178]</sup> Inverse control was implemented by iteratively updating the actuation state of one actuator at a time until the end effector reached the desired position. By making the assumption that the dynamics of soft robots are slow, Largilliere et al.<sup>[179]</sup> created a multilevel simulation approach that performed the

computationally expensive calculation of the stiffness matrix of the robot at a rate of 15 Hz and solved the inverse problem to define the actuation states at a rate of 600 Hz (**Figure 5a**). This approach reduced errors in the controls, but is applicable only to actuators that satisfy the assumption of slow dynamics, such as large pneumatic actuators. The assumptions of linear elasticity and small numbers of nodes in these works limit the accuracy of the simulations and the complexity of the robots that can be simulated (small number of nodes). FEM has been used to generate a reduced-order model that decreases the number of DOF.<sup>[159]</sup> It involves a very computationally expensive initial step to calculate many of the possible actuation states of the system. This database of states is subsequently used to inversely solve for the desired actuation state of the actuators. The approach is compatible with nonlinear materials' properties and relatively large numbers of nodes in the original FEM mesh (>15 000) while providing lower error and faster computational times.

Open-loop control is enhanced by analytical models that use knowledge of the actuator physics to predict the deformation of actuators. Modeling the deformation of soft materials is a key step in the development of these physics-based models. Elastomers are often represented using a hyperelastic model derived from strain energy density function.<sup>[180]</sup> The neo-Hookean model takes into account the deformation of an elastomer due to entropic elasticity and has only one materials

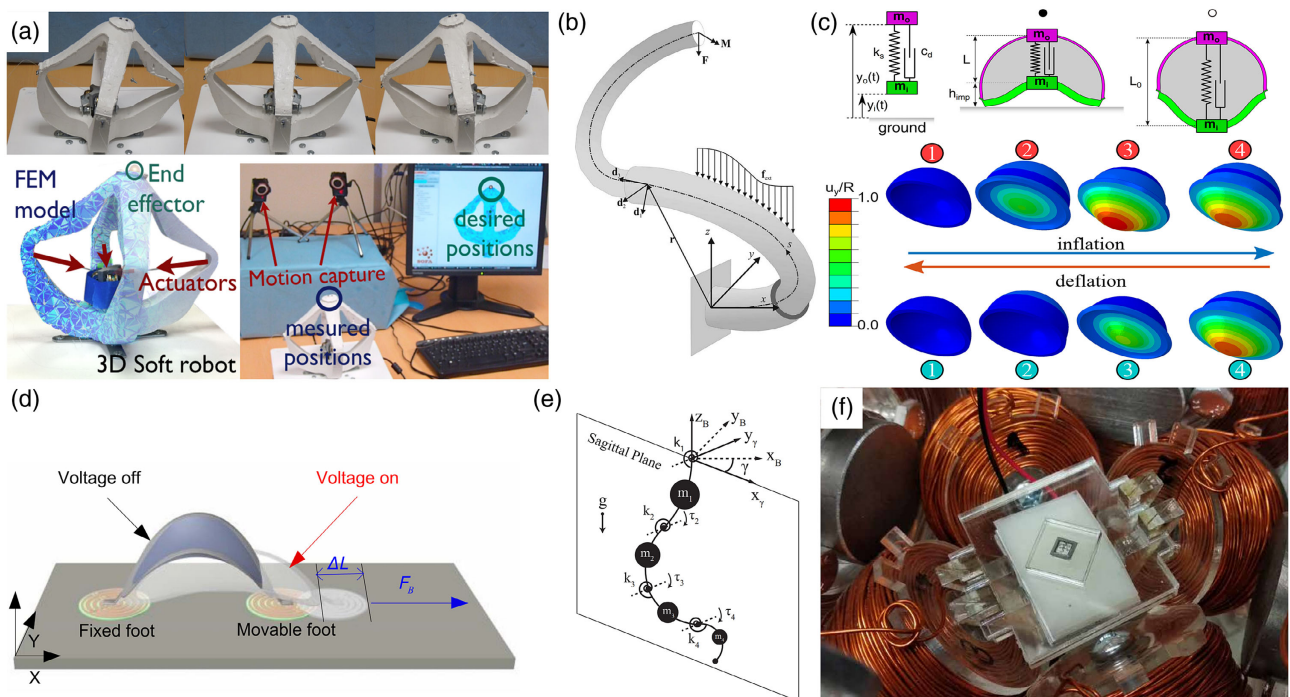


**Figure 5.** The implementation of open-loop control in different kinds of soft robots. a) Real-time FEM model control for a pneumatic soft robotic manipulator. Reproduced with permission.<sup>[178]</sup> Copyright 2013, IEEE. b) Fiber-reinforced model of the air muscle actuator coupled with dynamic model based on geometrically exact Cosserat rod theory. Reproduced with permission.<sup>[201]</sup> Copyright 2008, IEEE. c) Using both the physical model and FEM model to guide the control of the inflatable soft jumper. Reproduced with permission.<sup>[110]</sup> Copyright 2020, AAAS. d) Switch control of the electroadhensive wall-climbing robot. Reproduced with permission.<sup>[58]</sup> Copyright 2018, AAAS. e) Dynamic model and trajectory optimization for a multibody fluidic elastomer manipulator. Reproduced with permission.<sup>[115]</sup> Copyright 2016, SAGE. f) Open-loop control for millimeter-scale flexible robot driven by the magnetic field. Reproduced with permission.<sup>[214]</sup> Copyright 2019, AAAS.

parameter. It is generally accurate up to 100% tensile strain.<sup>[181]</sup> The strain stiffening that occurs at larger strains is taken into account by models that have two or more materials' parameters. Time-dependent effects are considered using a viscoelastic model composed of combinations of springs and dashpots<sup>[110]</sup> (Figure 5c) and their combinations: visco-hyperelastic models.<sup>[182]</sup> Actuators based on the deformation of elastomers include pneumatic actuators and DEAs. Analytical models for the deformation of pneumatic actuators have investigated the effect of fiber reinforcements<sup>[141,183]</sup> on single tube-like actuators and the effect of the geometry on the actuation characteristics of PneuNets composed of arrays of coupled bladders.<sup>[181,184]</sup> For DEAs, the electrical force can be considered as "electrostatic pressure," where the applied pressure is quadratically related to the electric field.<sup>[185]</sup> The deformation of DEAs can also be derived from energy considerations.<sup>[186,187]</sup> Analytical modeling of DEAs can be complicated by the viscoelastic properties of common DEA materials, but this can be compensated by the incorporation of appropriate viscoelastic models. For example, Gupta et al. developed a model that could predict the deformation of a highly viscoelastic DEA for up to 20 s.<sup>[188]</sup> The ionic transport of ionic actuators can be calculated by the Nernst–Planck equation.<sup>[189]</sup> Then, by using the derived ionic charge density, the strain of the actuator can be obtained by a diffusive elastic metal model where the material strain is proportional to the ionic charge density.<sup>[190]</sup>

Establishing an accurate phenomenological model for estimating the displacement of TCP involves two steps: 1) determining the electrothermal coupling of the resistor and (2) modeling the thermal–elastic behavior based on the geometry and the thermal expansion behavior.<sup>[191]</sup> The modeling of magnetic-driven robots combines the conventional kinematic model of soft robots with the application of magnetic forces. For example, the locomotion and deformation of a ferrofluid droplet are controlled using a kinetics model of a viscous ferrofluid combined with a magnetic force model.<sup>[192]</sup> The magnetic force/torque of dipoles was incorporated into the discrete elastic rod model to simulate a worm-like robot with embedded magnets.<sup>[193]</sup>

Since the kinematic and dynamic models are mathematical representations of the robot, the structure of the robot determines the choice of model. The equivalent lumped system model<sup>[194]</sup> assumes that soft continuum robots contain a highly articulated rigid link system with an infinite number of disks connected through spring-damper-supported spherical joints.<sup>[195]</sup> It uses the idea of finite element to make the model more accurate, but the computational complexity makes it difficult to implement to an online controller. The piecewise constant curvature (PCC) model<sup>[196,197]</sup> simplifies the description of the system and reduces the computational complexity significantly by approximating the structure as a constant curvature (Figure 5e). It has been widely used in soft continuum robots because its error is acceptable when the payloads are quite small and the gravitational effects can be eliminated when the robot works in a horizontal plane. It is compatible with open-loop control.<sup>[115,198]</sup> Integration with a feedback controller enables more advanced systems.<sup>[116,199]</sup>

The variable curvature (VC) hypothesis assumes that the soft robot consists of a series of segments with constant curvature.<sup>[200,201]</sup> For example, the Cosserat rod model provides a

mathematical framework that accommodates all six possible DOFs to formulate the dynamics of rods. Combined with discrete computational methods, many scenarios in soft robots such as elastic filaments,<sup>[202,203]</sup> continuum robots,<sup>[204]</sup> and octopus-like robot arms<sup>[205]</sup> can be solved accurately. By allowing additional DOF of extension and shearing, the Cosserat rod model can take multiple physical effects into account,<sup>[203]</sup> such as the nonlinear mechanical properties of elastomers<sup>[206]</sup> and a physical model for reinforcing fibers.<sup>[207]</sup> The Cosserat rod model works well for systems that are composed of long and slender components, which has made it useful to model the deformation of biological systems that are composed of bones and bundles of muscles fibers.<sup>[208]</sup> Recent innovations in fabrication and 3D printing have made available a range of fiber-like actuators compatible with Cosserat rods. For example, DEAs and LCEs have traditionally been fabricated in planar geometries, but have recently been fabricated using 3D printing.<sup>[32,132]</sup>

The computational complexity of these numerical methods is a barrier to achieve online control with feedback. However, by using the Ritz and Ritz–Galerkin method, real-time online control can be achieved.<sup>[209]</sup> The continuum approximation of hyper-redundant systems<sup>[112,210]</sup> and the spring–mass model<sup>[211]</sup> also possess the drawback of high computational complexity. The continuum approximation of hyper-redundant systems is suitable for modeling continuum structures with small deformations such as robotic snakes<sup>[210]</sup> and trunk manipulation.<sup>[112]</sup> The spring–mass model needs to be calibrated experimentally for every new design.

For magnetic-driven actuator mechanisms, open-loop control can be achieved by controlling the field manually<sup>[82,212]</sup> or changing the direction according to a certain pattern.<sup>[80]</sup> With the development of multi-material 3D-printing technology, the polarization of each pixel in a printed structure can be programmed. These programmed structures can realize diverse motions of untethered magnetic actuators by manual stimulation using permanent magnets.<sup>[82]</sup> For tethered continuum robots with the same fabrication technology, their motion can be controlled by changing the direction of the magnetic field because the response of the inner ferromagnetic domains to external magnetic fields is denoted analytically.<sup>[213]</sup> To achieve more accurate and complicated behavior, creating a coil system that can generate a multidimensional uniform magnetic field or magnetic gradient field is necessary (Figure 5f).<sup>[214]</sup> The coil system usually contains two types of coils: Helmholtz coil and Maxwell coil. The Helmholtz coil consists of two identical coils arranged on the same axis and is able to generate a uniform magnetic field near the center. The Maxwell coil consists of two coils with current flowing in opposite directions, which creates a gradient field close to the center of coils.<sup>[215]</sup> Here, H-M magnetic navigation system consists of a Helmholtz coil and a Maxwell coil that are arranged coaxially to generate 2D magnetic fields.<sup>[216]</sup> An improved structure that possesses three fixed orthogonal Helmholtz coils, a stationary Maxwell coil, and a rotatable Maxwell coil has the ability to achieve 3D locomotion with the drilling of a microrobot.<sup>[217]</sup> Meanwhile, the magnetic-torque-driven systems only contain several orthogonal Helmholtz coils to generate a rotating or oscillating magnetic field, which are able to apply magnetic torque to microrobots in fluidic environments. The OctoMag system is another typical coil system whose coils

are no longer all orthogonal. It has eight coils all pointing to one center. Four of them are set downside horizontally while another four are set upside with a tilted angle of 45°. A full 5-DOF control is enabled by this kind of coil system.<sup>[93]</sup>

While on/off switch control is not strictly a control system, it will be briefly described here due to its widespread use in practical robotic systems.<sup>[58,104,106,218,219]</sup> Switch control is commonly used for actuators that only have two states, on or off. For example, EA<sup>[58]</sup> devices are usually operated using two states: adhesion and no adhesion (Figure 5d). Some actuators have highly nonlinear deformation processes, such as SMA, MSMA,<sup>[98]</sup> TCP,<sup>[220]</sup> and magnetorheological elastomer (MRE).<sup>[221]</sup> For these nonlinear actuation mechanisms, it can be difficult to develop a physical model to describe the continuous change, so on/off switch control focuses on the initial and final state of the actuation. Another situation in which switch control is valuable is when the deformation of a robot is achieved by many small actuators. Then, on/off switch control of the small actuators can achieve a range of deformation states of the overall robot. For fluidic-driven actuator mechanisms, accurate control of the displacement and force can be achieved by sophisticated pressure controllers.<sup>[22,222]</sup> However, switch control is still popular since low-cost solenoid valves commonly offer only two operational states: on and off. In the "direct way" of electric-driven actuator mechanisms, such as DEAs<sup>[223]</sup> and piezoelectrics,<sup>[218,224]</sup> high-voltage transistors are often difficult to implement into small structures, so simple relays are often used that only allow on/off control. Complex motions can be formed by arranging different switches.<sup>[106]</sup>

For a legged robot, different motion types of the entire robot can be achieved when switch control of its actuators is implemented in a specific order.<sup>[225]</sup>

## 4.2. Closed-Loop Control

The implementation of first-level closed-loop control focuses on the mechanisms for monitoring the actuation of different actuator mechanisms. For example, feedback about the internal state of fluidic-driven soft robots is usually achieved by internal pressure or flow sensors.<sup>[127,128]</sup> However, since the valves are bulky and expensive, it is difficult to precisely control the pressure or flow rate of air inside each actuator. An alternative method is to measure external variables such as strain,<sup>[133]</sup> force,<sup>[135,226]</sup> and flexion<sup>[120]</sup> (Figure 6a) to form a closed-loop control system.

The first-level closed-loop control of direct way of electric-driven actuator mechanisms can be achieved using self-sensing algorithms without any additional sensors. In DEAs, self-sensing relies on measuring the voltage or current to sense the DEA's capacitance or electrode resistance, which can lead to the estimation of the force and displacement of DEAs (Figure 6c).<sup>[129,130,227,228]</sup> However, converting this self-sensed signal into a displacement requires the use of a model, which can be inaccurate in the presence of external perturbations. The self-sensing system provides an estimate, while more precise feedback about the status of the system can be obtained from external sensors. Hence, even though integrating external sensors, such as strain sensors,<sup>[34]</sup> displacement sensors,<sup>[229]</sup>

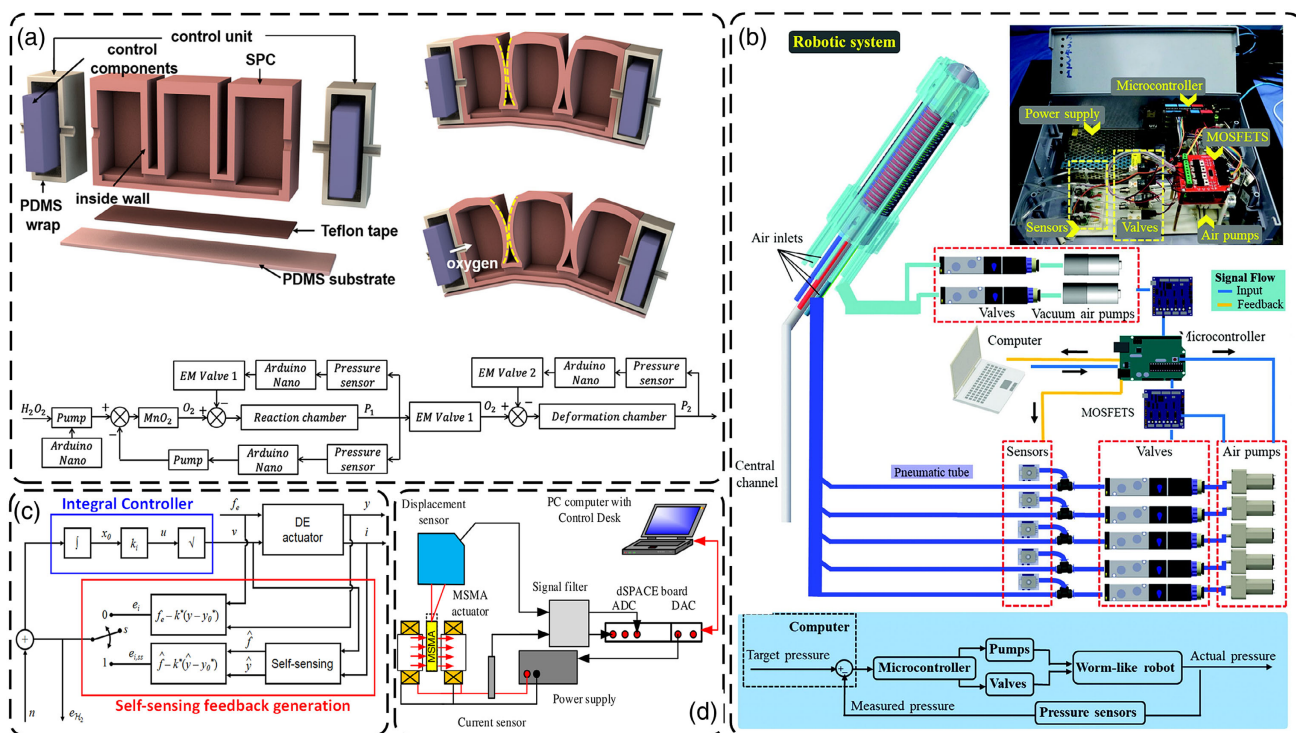


**Figure 6.** First-level closed-loop control of soft robot systems a) Pneumatic closed-loop control system for a one-DOF untethered soft chemomechanical actuator. Reproduced with permission.<sup>[127]</sup> Copyright 2019, Elsevier. b) First-level closed-loop control of the pneumatic system for a worm-like soft robot. Reproduced with permission.<sup>[351]</sup> Copyright 2019, Mary Ann Liebert, Inc. c) Self-sensing stiffness control diagram for DEAs. Reproduced with permission.<sup>[130]</sup> Copyright 2019, IEEE. d) Control diagram for MSMA actuators. Reproduced with permission.<sup>[236]</sup> Copyright 2019, IOP.

and cameras<sup>[118]</sup> increase the system cost and size, better accuracy of the control can be obtained.

The self-sensing method established for SMA and TCP actuators can accomplish an accurate estimate of strain by measuring the resistance or temperature.<sup>[230–232]</sup> Using external position<sup>[233]</sup> and pressure,<sup>[234]</sup> sensors are widely used to achieve single and dual closed-loop control.<sup>[231]</sup> Since the first-level control of tendon-driven soft robots (electromagnetic motor<sup>[62]</sup> and piezoelectric motor<sup>[63]</sup>) can be readily realized by integrated encoders, self-sensing methods are already built into the actuator, so development efforts focus on the second level control.

In addition to the sensing methods, the physical model of actuator mechanisms plays an important role in first-level closed-loop control. While first-level controllers often use control algorithms that are agnostic to the actuator mechanism (e.g., proportional-integral-derivative (PID) control), tailoring the model to the actuator mechanism can improve the quality of the control. For example, most control algorithms are linearized, while DEAs exhibit a quadratic dependence between the voltage and the displacement. Incorporating this quadratic relationship into the control system improves the accuracy.<sup>[235]</sup> First-level closed-loop control can also compensate for the viscoelasticity of DEA materials.<sup>[108]</sup> Similarly, the modeling of MSMA actuators can be

improved by including the effects of hysteresis (Figure 6d).<sup>[236]</sup> Model-based closed-loop control for fluidic-driven actuators possesses higher performance since the relationship between pressure and actuation (bending<sup>[237]</sup> or linear motion<sup>[22,238]</sup>) is depicted. The simplified physical model can provide a stage for model predictive control (MPC) in the joint space of a pneumatic soft robot arm (Figure 6b).<sup>[119]</sup>

The WPT controller introduced in Section 2.3 requires a composite signal with multiple frequencies to stimulate multiple actuators simultaneously, but collecting feedback from the actuators is a challenge. The work of Wang et al.<sup>[239,240]</sup> proposes a closed-loop control method for wireless control using the discrete form of a composite signal. The approach was applied to a delta robot with three motors, achieving a simple trajectory tracking task.

The primary function of the second-level control loop is to relate the configuration or task space to the joint space outputs. Therefore, it requires developing a model for the entire robot body rather than a single actuator or end effector. Thus, the key step in this control strategy is the development of a mathematic kinematic and dynamic model (Figure 7b).<sup>[123,125,241,242]</sup>

The measurement strategy is determined by the size and structure of the robot. For example, microsize devices, such

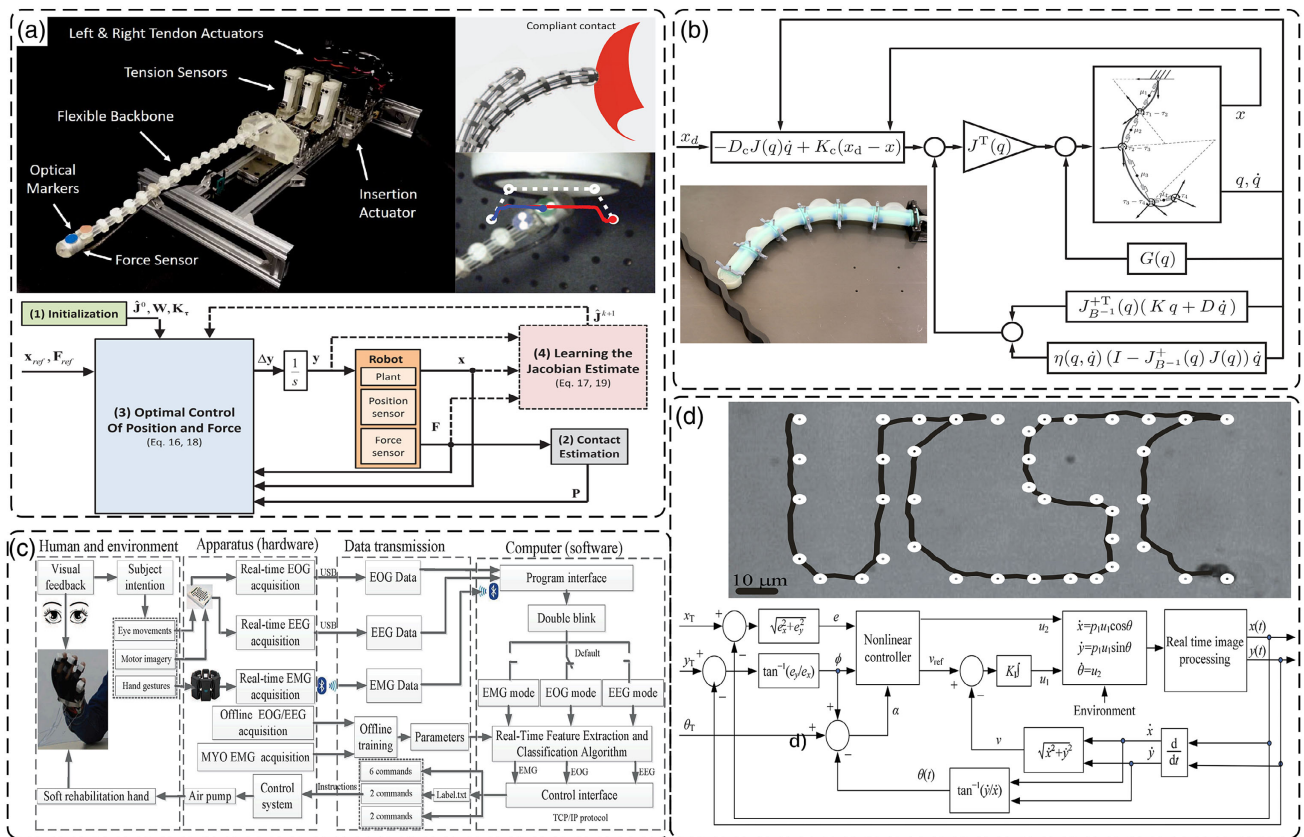


**Figure 7.** Second-level closed-loop control of soft robot systems. a) Model-less closed-loop hybrid position/force control of tendon-driven continuum soft robot in the task space. Reproduced with permission.<sup>[142]</sup> Copyright 2016, IEEE. b) Model-based dynamic closed-loop control of a planar pneumatic soft robot with abilities including trajectory tracking and interaction with the environment. Reproduced with permission.<sup>[123]</sup> Copyright 2020, SAGE. c) A real-time control of pneumatic soft robot hand based on EOG, EEG, and EMG as input and human visual as feedback. Reproduced with permission.<sup>[124]</sup> Copyright 2019, Frontiers. d) Second-level closed-loop control of magnetic microswimmer based on the visual feedback. Reproduced with permission.<sup>[243]</sup> Copyright 2017, Springer.

as magnetic microrobots<sup>[126,243]</sup> (Figure 7d) and biological cells<sup>[244]</sup> must use a vision system to provide feedback since no onboard sensors are small enough to be integrated into such micron-scale robots. Larger actuators driven by fluid,<sup>[245]</sup> electricity,<sup>[125]</sup> and WPT systems<sup>[239]</sup> can use diverse sensors to provide feedback for the second-level control, including contactless cameras<sup>[246]</sup> and integrated electromagnetic sensors.<sup>[245]</sup> Input signals from human beings,<sup>[124]</sup> (Figure 7c) can provide bionic feedback.

#### 4.3. Autonomous Control

Most electric-driven soft robots have relied on conventional rigid electronics to implement onboard autonomous control<sup>[37]</sup> since they can store the program, process the algorithms, and even provide power in a small area. However, achieving completely soft robots can be enabled by stretchable electronics, which is a rapidly progressing field.<sup>[247–250]</sup> For electronic actuators that use transistors to control high voltages, the development of integrated flexible or organic transistors provides new opportunities for onboard autonomous control.<sup>[251–254]</sup> For fluidic-driven soft robots, in addition to the rigid<sup>[255]</sup> or stretchable circuits<sup>[256]</sup> that can execute the control algorithms, the system requires miniaturized valves and reliable onboard power sources (compressed air source or chemical decomposition).<sup>[28,257,258]</sup> When it comes to magnetically driven soft robots, because the energy source is a field source, the power and control are driven directly by the magnetic field.<sup>[259,260]</sup> Therefore, there is no need to mount a bulky power source or wired connection to any remote source, which is an enormous constraint for other soft robots to achieve onboard control.

In soft robots, an adaptive controller<sup>[261]</sup> for continuum manipulators can provide asymptotic tracking of desired joint

trajectories through dynamic parameter modification.<sup>[262]</sup> By using online learning methods, kinematic model parameters of a double-joint robot finger can be obtained iteratively to enable an adaptive controller<sup>[120]</sup> (Figure 8a). Also, for soft grippers, the grasping force regulation in the presence of unknown contact mechanisms can be achieved by an adaptive neuro-fuzzy system (ANFIS).<sup>[263]</sup>

MPC is a model-based autonomous control strategy in which the control input is optimized over a set time horizon, applied for a single timestep, and then optimized again. This process is iterated to minimize a predefined cost function.<sup>[264]</sup> While it has traditionally been used for industrial processing, the improvement of computing power and optimization algorithms has increased the control rate to be compatible with soft robotics applications. For example, the CVX-GEN, a web-based tool for developing convex optimization solvers, is used for solving the optimization problem of the MPC controller of soft robots (Figure 8b).<sup>[119]</sup> The nonlinear control problem of soft robots can be linearized using a controller designed for its linear Koopman representation.<sup>[265]</sup> Traditional MPC for pneumatic actuators utilizes linearization and estimation of the higher order unknown terms to treat nonlinear features, which sacrifices the accuracy and frequency of the control system. Thus, using neural network-based methods can be an alternative solution for nonlinear MPC.<sup>[266,267]</sup>

Autonomous control without any predefined model requires empirical estimation<sup>[268]</sup> or ML-based data-driven model generation.<sup>[269]</sup> With the advancement of ML algorithms and the popularity of open-source platforms, ML algorithms with lower barrier to entry have become mainstream in this area. In most cases, ML algorithms implemented in model-free controllers typically utilize mature software platforms (Machine Learning and Deep Learning Toolbox of MATLAB or Scikit-learn of Python). Consequently, the key challenge is the generation of

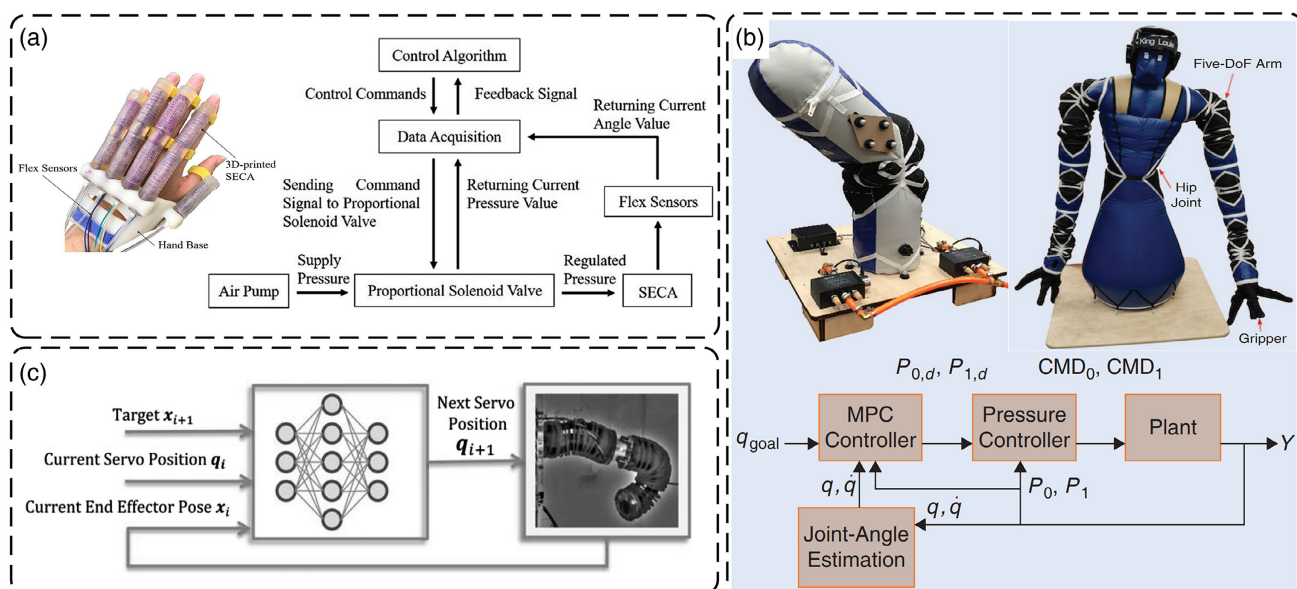


**Figure 8.** Autonomous control of soft robot systems a) Pneumatic adaptive control system for a single actuator of a soft glove. Reproduced with permission.<sup>[120]</sup> Copyright 2021, SAGE. b) MPC controller implemented in a single pneumatic joint of a five-DOF soft arm. Reproduced with permission.<sup>[119]</sup> Copyright 2016, IEEE. c) ML-based learning closed-loop kinematic controllers for continuum manipulators. Reproduced with permission.<sup>[269]</sup> 2019, Mary Ann Liebert, Inc.

data sets used to train the algorithms. Hysteresis or poor repeatability in some soft actuators can inhibit the ability to generate high-quality datasets. For example, ionic actuators can exhibit time-dependent actuation properties and performance changes due to drift or changes in ambient conditions (e.g., humidity). Consequently, actuating a single array of devices many times can result in datasets that are difficult to reproduce.

The data inputted in the training process depends on the level of the control system. In the joint space, data from sensors that indicate the joint deformation is used as input into the ML algorithms. By using regression models, raw sensors<sup>[270]</sup> or matrix sensors<sup>[271]</sup> can be calibrated with real-world values. ML approaches are particularly useful in situations in which the internal coupling or nonlinear behavior of a system is too complex to be understood using analytical models. In the configuration space and task space, ML algorithms are used to learn the kinematic and dynamic models while the sensors and actuator mechanisms located in the first level become abstract. If the system is treated as quasistatic, which means it reaches static equilibrium in each control step, only the kinematics need to be considered. The key challenge for these kinematic models is to find the global representation of the Jacobian. Even though some analytical models have been introduced in open-loop control, their accuracy is limited by simplifying assumptions. In contrast, ML algorithms avoid making any simplifying assumptions, allowing them to accurately capture the behavior of the robotic system.

In addition to neural networks, the most basic form of ML algorithm, the global Jacobian can also be obtained using advanced forms of ML algorithms such as linear function approximators,<sup>[272]</sup> constrained extreme learning machines,<sup>[273]</sup> and ensembles of neural networks.<sup>[274]</sup> The mapping of the virtual global Jacobian can be obtained by performing gradient descent over the actuator configuration with the desired position as the target without deducting any models in robotics. However, the undefined motion iteration in the robot between each commanded position induced by such ML algorithms will potentially cause slower execution of the controller.<sup>[275]</sup>

Complex dynamic models can be learned by ML algorithms without any preparatory knowledge.<sup>[276]</sup> Also, ML algorithms can evolve existing dynamics models. For example, learned dynamic parameters can increase the precision of the stiffness and position control of the soft actuators,<sup>[277]</sup> while dynamic models with varying parameters such as stiffness-tuning soft manipulators can use ML algorithms to achieve the adaption.<sup>[278]</sup> By implementing the neural network in the control structure, rigid robots can learn to achieve target motion with reduced numbers of control inputs.<sup>[279]</sup> It is more challenging to implement similar algorithms in soft robots because the actuator mechanisms are diverse and the robots exhibit more complex motion.

For tethered robot systems, the joint space can be distinguished with configuration and task space since the actuators need to be mounted on the base and the tasks are finished by the end-effector. Thus, the implementation of these methods often relies on the ML algorithm integrated into the dynamic and kinematic model of the robot.<sup>[152,155,156]</sup> Meanwhile, for untethered robot systems, the concept of an end-effector no longer exists. There is no obvious difference between joint space and

task space. To this extent, the characteristics of actuator mechanisms have a direct impact on the control algorithm.<sup>[280,281]</sup>

#### 4.4. Summary

The following four aspects, “Actuator, Model, Sensor, and Controller,” will affect the control system. Here, the actuator mechanisms and control strategies have been described in Sections 2 and 3. Figure 8 shows a conceptual map of the main categories of soft robot control strategies. Due to the limitation of space, some detailed categories are not shown. We highlight eight papers as examples of works that have selected different combinations of actuators, models, sensors, and controllers (**Figure 9**).

From Figure 8, except for the classifications mentioned in this article, the implementation route of each case is represented by dotted lines. To illustrate such routes, the detailed information of each example is shown in the legends. At present, most soft robot systems can be represented as an implementation route on this diagram.

### 5. Emerging Directions

The development of materials science has enabled unprecedented levels of integration between the controller and actuator. To meet the requirements of complex actuation, soft robots increasingly have multiple actuators with independent control. Example multi-actuator systems include a bionic robot hand<sup>[38]</sup> (**Figure 10a**), hexapod robot<sup>[223]</sup> (**Figure 10b**), programmable surface<sup>[36]</sup> (**Figure 10c**), modular robot<sup>[282]</sup> (**Figure 10d**), swarm robot<sup>[283]</sup> (**Figure 10e**), and continuum soft robot<sup>[284]</sup> (**Figure 10f**). However, the increase in the number of individual actuators will increase the dimensions and weight of the control system, which is contradictory to the trend of miniaturization. Thus, to solve this contradiction, an underactuated control system is desired, which refers to the ability to control more actuators with fewer control signals. Methods to achieve underactuated control will be discussed in this section. In addition, the emergence of AI has enabled new opportunities in soft robotics since intrinsic models and traditional controllers can be replaced or improved by ML algorithms. However, for soft robots, the implementation of AI is not limited to algorithms, but can be incorporated into the materials and devices.

#### 5.1. Interfacing Between Controller and Actuator

There is a myriad of different applications for soft robots that require different control capabilities (types of feedback, time response of feedback, etc.) and actuator characteristics (bandwidth, actuation stress, etc.). Designing the optimal robot for a task could benefit from the use of a particular type of actuator mechanism with a control system that may have a different energy source or materials set. For example, biological muscles combine the high energy density of chemical energy and the fast response of electronic controls (nerves). Progress in soft materials and their fabrication methods<sup>[285]</sup> has enabled new strategies to combine different energy sources and actuation mechanisms in a way that broadens the control strategies that can be achieved.

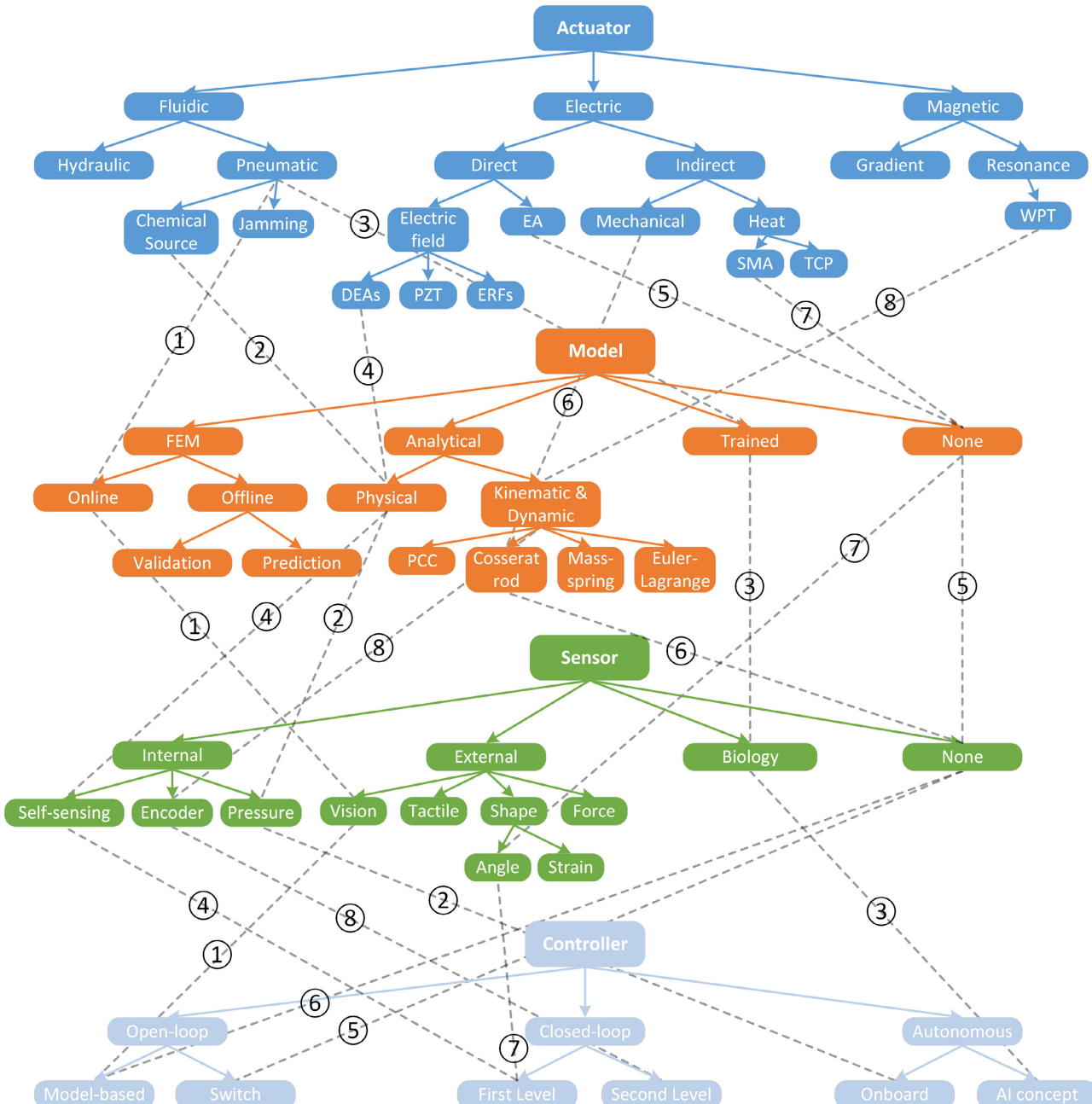


**Figure 9.** The implementation diagram for diversified soft robot systems with several typical examples. 1) Pneumatic actuator→Online FEM model→External vision measurement→Model-based open-loop control.<sup>[178]</sup> 2) Pneumatic actuator based on chemical source→Physical analytical model→Internal pressure sensor→Autonomous onboard control.<sup>[28]</sup> 3) Pneumatic actuator→Trained model→Biology sensor(EOG/EEG/EMG)→Autonomous control with AI concept.<sup>[124]</sup> 4) DEAs→Physical analytical model→Self-sensing→First level closed-loop control.<sup>[130]</sup> 5) EA→No model→No sensor→Switch open-loop control. 6) Tendon-driven actuator→Cosserat rod-based kinematic model→No sensor→Model-based open-loop control.<sup>[352]</sup> 7) SMA→No model→External angle sensor→First-level closed-loop control.<sup>[233]</sup> 8) WPT based magnetic-driven actuator→Kinematic model of parallel robot→Internal encoder→Second-level closed-loop control.<sup>[239]</sup>

The diagram in **Figure 11** shows a simple closed-loop feedback structure. The model, consisting of mathematical algorithms, is usually executed in a computer chip, the output of which is compatible with electronic controllers. In addition, electronic control signals possess advantages of high speed and compatibility with multiplexing methods. The value of electronic control systems is

emphasized by the observation that electronic controls (nerves) have evolved in all complex animals despite the fact that biomaterials have inherently poor electrical properties. Electronic control of electronic actuators has been developed extensively for decades. (Figure 11a) However, new strategies are being developed to implement electronic control strategies

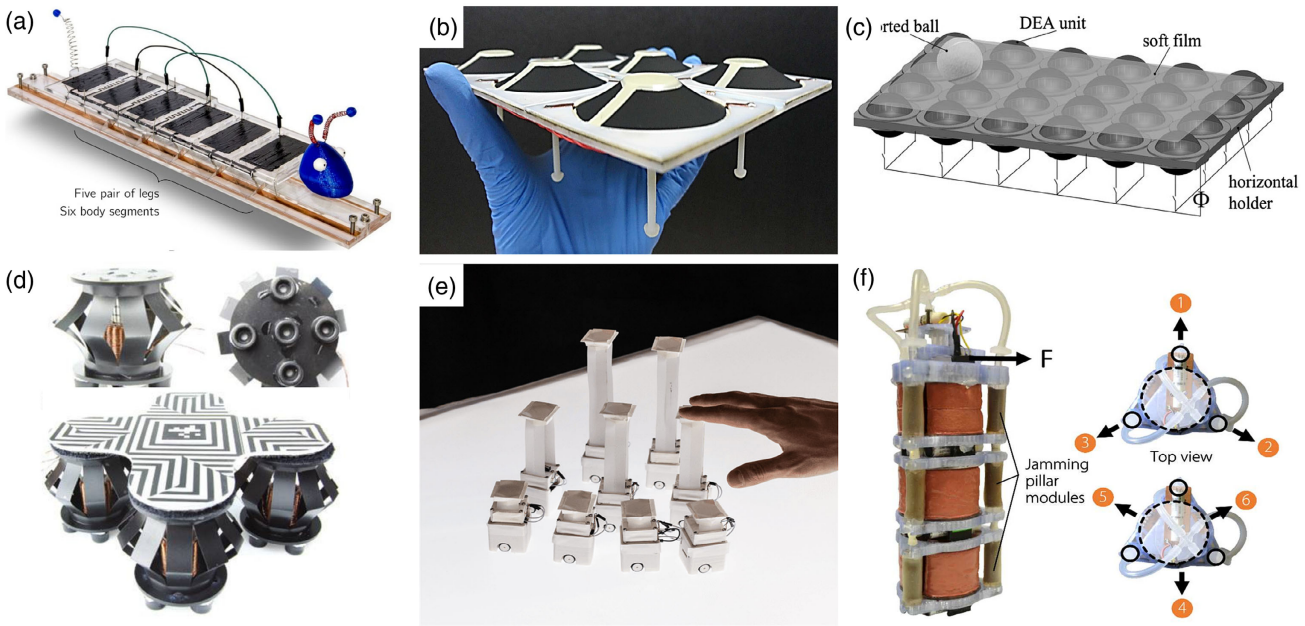


**Figure 10.** Typical multiactuator soft robot systems. a) Bionic soft robot with multiple motion DOFs driven by DEAs. Reproduced with permission.<sup>[38]</sup> Copyright 2017, Mary Ann Liebert, Inc. b) Printable monolithic hexapod robot driven by soft actuators. Reproduced with permission.<sup>[223]</sup> Copyright 2015, IEEE. c) Programmable surface driven by matrix DEAs system. Reproduced with permission.<sup>[36]</sup> Copyright 2017, Mary Ann Liebert, Inc. d) A module untethered soft robot that can be reconfigured to achieve multiple tasks. Reproduced with permission.<sup>[282]</sup> Copyright 2020, Mary Ann Liebert, Inc. e) Shape-changing swarm robots with soft structure. Reproduced with permission.<sup>[283]</sup> 2019, ACM. f) Continuum soft robot with vacuum-powered soft pneumatic actuator. Reproduced with permission.<sup>[284]</sup> 2017, AAAS.

in diverse actuator mechanisms. For example, embedding heating wires can enable electro-actuation based on the thermal-responsive behavior of LCEs and shape memory polymers.<sup>[66]</sup> (Figure 11d) Hydraulically amplified self-healing Electrostatic (HASL) actuators employ an electronic energy source and electronic controls to deform a pouch filled with dielectric liquid (Figure 11f).<sup>[286,287]</sup> It can be seen as a method to combine the advantages of hydraulic actuators with the advantages of electronic control systems. The free-flowing nature of the hydraulic component of the actuator allows the application of force and deformation in a different location than where the electrical energy is applied.<sup>[288]</sup> A traditional hydraulic actuator would require a controller, pump, and pressure or deformation sensor to achieve closed-loop feedback, but HASL actuators can provide power, controls, and self-sensing feedback using a simple pair of electrodes.<sup>[286]</sup> Soft pumps based on electrostatic forces<sup>[289]</sup> similarly use electronic controls and power but with an unclear route towards self-sensing feedback.

The traditional method to control magnetic robots consists of either manually moving magnets or switching an electromagnet on and off. Magnetic microrobots typically have fixed functionality based on the preprogrammed form of the robot that is related to the spatial distribution of the magnetically active components. Facilitated by electrical coil systems that can be programmed to generate time-varying fields, complex motion such as trajectory tracking can be achieved (Figure 11b).<sup>[214]</sup> By incorporating electromagnets into a soft robot, the coupling between the robot and the external field can change the control strategy from external control using vision systems to on-board control,

(Figure 11c).<sup>[177]</sup> Compared with the traditional method, this novel interfacing way allows larger dimension robots and potentially enable self-sensing control.

Joule heating of low-boiling-point liquids induces the evaporation of the liquids to expand a chamber, enabling very large volume changes. This can be seen as an electrothermal method to activate and control devices that have similar characteristics to pneumatic actuators. This method of electronic control of pneumatic actuators could be compatible with closed-loop feedback methods that measure either the temperature change or the deformation change (Figure 11g).<sup>[290]</sup>

While electrical control of actuators has advantages, one of the key limitations is the use of an electrical power source such as a battery, which is typically heavy and is not yet soft. Solid electronic controllers inevitably affect the “soft” mechanical properties of soft robots. Therefore, implementing pneumatic (or hydraulic) controllers that can achieve digital logic operation based on soft materials without electronics is an area for opportunity. For example, soft, pneumatic digital logic gates that generate known pneumatic outputs as a function of one, or multiple, pneumatic inputs allows pure soft robots to achieve onboard control with a complex algorithm without any electronics (Figure 11h).<sup>[139,291]</sup> Reducing the dimensions of fluidic logic gates is a key step to make this approach practical.

## 5.2. Addressing

As the number of actuators and sensors within a robot increases, getting electrical signals into and out of the devices becomes a

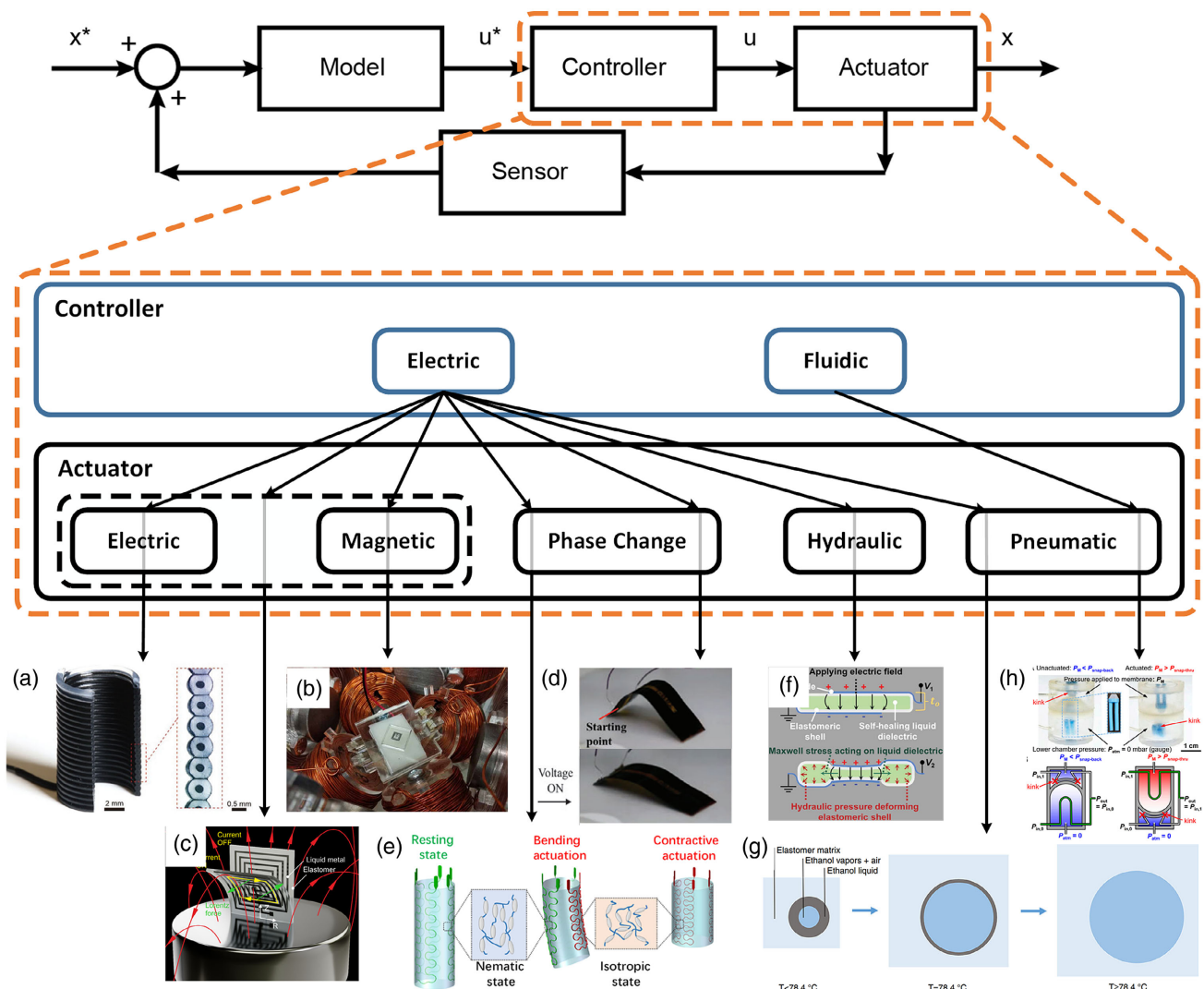


**Figure 11.** Interfacing between controller and actuator. a) Multicore-shell 3D printing DEAs driven by electrostatic field can achieve complex shape morphing responses. Reproduced with permission.<sup>[32]</sup> Copyright 2021, Wiley. b) Programmable motion of magnetic-driven soft robot achieved by electric-controlled coil system. Reproduced with permission.<sup>[214]</sup> Copyright 2019, AAAS. c) Shape-morphing system based on soft electromagnetic actuator is controlled electrically. Reproduced with permission.<sup>[177]</sup> Copyright 2020, AAAS. d) An electroactuated SMP actuator based on its thermal-responsive behavior. Reproduced with permission.<sup>[66]</sup> Copyright 2020, Mary Ann Liebert, Inc. e) Electrically controlled temperature phase change soft tubular actuator based on LCE. Reproduced with permission.<sup>[353]</sup> Copyright 2019, AAAS. f) Peano-HASEL actuator whose actuation is realized with the assist of liquid is driven by electrostatic field. Reproduced with permission.<sup>[286]</sup> Copyright 2018, AAAS. g) A pneumatic actuator potentially driven by the electrothermal method. Reproduced with permission.<sup>[290]</sup> Copyright 2017, Nature. h) Pneumatic digital logic controller for pneumatic soft robots. Reproduced with permission.<sup>[291]</sup> Copyright 2019, PNAS.

challenge for which new innovations are being pursued. Direct addressing refers to the connection of wires to each of the active devices. For a two-terminal device such as an electrothermal actuator,  $2 \times n$  wires are required to control  $n$  devices. Direct addressing is attractive in its ability to provide control signals, power, and feedback signals (e.g., self-sensing of DEAs) through one set of connections. Many biological functions are based on direct addressing, including data collection from stretch sensors that enable proprioception and the activation of muscles by nerves. In biological systems, direct addressing is effective because: 1) nerves are very small, and therefore hundreds of nerves can fit within a bundle, 2) most biological functions are

one-terminal, which means that  $n$  nerves are required to collect information from  $n$  sensors (most electronic devices have two or three terminals), and 3) the 3D distribution of nerves and active devices relaxes the geometric constraints on wiring pathways. In traditional 2D electronics, the number of devices that can be connected using direct addressing can be limited by the wiring complexity.<sup>[292,293]</sup> However, the advent of 3D printing enables 3D arrangements of wiring interconnects,<sup>[32,294]</sup> opening the door to bio-mimetic scalability using direct addressing.

Multiplexing refers to any strategy that reduces the number of wires needed to address an array of devices. The development of soft actuator arrays can take inspiration from the long history

of multiplexing strategies used in electronics, such as organic LED displays in cell phones and sensor arrays in electronic skin.

Some nerves in the body carry information from multiple sources. For example, nerves in the skin collect sensory information from multiple pressure sensing cells and convey that information in a series of voltage pulses. In this way, information from a large number of sensors can be collected using a single wire (neuron).<sup>[295]</sup> This concept has inspired the development of sensor networks with minimal wiring complexity.<sup>[296]</sup> In time-division multiplexing (TDM), discrete control signals separated by short intervals are sent over a single communication wire and a circuit at the receiving end de-multiplexes the signals. This is a robust technological approach that has been developed extensively in the communications and sensing community. Direct implementations of these approaches have enabled soft robots that pace and bound<sup>[297]</sup> and robots and sensor networks with modular expandability.<sup>[298,299]</sup> However, implementing TDM in soft robots presents unique challenges. First, the demultiplexing must be done by high-performance electronics that can add to the bulk and complexity of the robot.<sup>[255]</sup> Second, TDM only provides control signals, and the power source for actuation must be supplied separately. Incorporating the control signals, electrical power, and fluid source into one bus line<sup>[284]</sup> can enable simplified and miniaturized fluidic actuator arrays.

Space-division multiplexing (SDM) refers to the use of separate point-to-point electrical conductors for each transmitted channel. Passive matrices use a crossbar architecture in which strips of electrodes oriented in the x-direction underneath a device and in the y-direction on top of a device allow the selective activation of one pixel of an array at a time. To address an  $n \times n$  array of devices, a passive matrix requires  $2 \times n$  connections, which dramatically reduces the number of connections for large arrays of devices (compared to direct addressing). However, the limitation of passive matrices is that the pixels must be addressed sequentially so the duty cycle during which each pixel is active is  $1/n^2$  in traditional passive matrices or  $1/n$  for more sophisticated multiplexers.<sup>[300]</sup> For sensors, a low duty cycle means that the sensor state is read out intermittently, which is not typically a problem. In actuators, one approach to overcome the limitation of intermittent power supply is to combine one layer of a global electrostatic actuator with a layer of shape memory polymer that can be locally addressed using a matrix.<sup>[301]</sup> The matrix is then used to modulate the global actuation of the electrostatic actuator. In this case, the actuation and addressing are accomplished by two different actuation mechanisms. However, actuators based on mechanisms such as reversible chemical reactions<sup>[302]</sup> could provide both functionalities in a single device. Active matrices refer to crossbar architectures in which a transistor is used in each pixel to improve the scanning rate and reduce the crosstalk between pixels. Recent innovations in stretchable transistor arrays could enable future large-scale arrays of soft actuators.<sup>[251,303]</sup>

Frequency-division multiplexing (FDM) refers to the process of sensing different control signals at different frequencies. In a broad sense, the bandpass hydraulic valves that only allow fluid to pass in a certain pressure range can control multiple actuators with only one fluid input, which can be considered as an FDM approach to drive fluidic actuators.<sup>[304]</sup> With the

development of WPT systems based on magnetic coupling resonance, WPT-based FDM is increasingly applied in electric-driven soft robots.<sup>[103,104,239,305,306]</sup> As mentioned in Section 2.3, WPT-based FDM can transmit the power and control signal simultaneously and wirelessly, removing the need for wires and onboard power. Since the TDM can only communicate with one actuator at one time, when the quantity of actuators increases, the time delay can no longer be ignored. Therefore, the WPT-based FDM provides a unique value proposition by enabling high-speed control of miniaturized robots. However, this is a nascent field, and current systems only show the ability to control three–four actuators simultaneously, which is sufficient for only basic movements. This number is limited by the nonideal capabilities of the receiving LC coil to respond selectively to only one frequency. Each LC coil contains smaller absorption peaks at frequencies other than the primary resonance, making it infeasible to choose a large amount of totally independent frequencies. In addition, miniaturizing the LC coil causes a decrease of the Q-factor (increasing the width of the absorption peak), which further makes frequency selection difficult. Another drawback of the WPT approach is the distance limitation. If accurate motion is required, such as the delta robot application,<sup>[239]</sup> the distance should be fixed at a specific optimized value. When precision is less important, a large ranger range of distances can be tolerable.<sup>[104]</sup>

### 5.3. Selective Control in Field Energy Source

Unlike the multiplexing control which is a kind of single-input multi-output control (SIMO), selective control using an electrostatic or magnetic field can typically drive one actuator at one time. Therefore, one of the key opportunities is to increase the number of actuators that can be addressed by one field, increasing the controllable DOF in these systems. Selective control can be achieved using field modulation,<sup>[307–310]</sup> frequency selectivity,<sup>[94]</sup> polarization selectivity,<sup>[311]</sup> or wavelength selectivity.

The field's properties can be modulated according to several sources of information input. For example, independent control of microrobots can be achieved by measuring the by identifying the unique velocity response of each microrobot in the field.<sup>[307]</sup> Alternatively, multiple magnetically different microrobots can be identified by using a single global rotating magnetic field. By exploiting the differences in their magnetic properties, different swimming behaviors can be triggered by controlling the frequency and the strength of the global field.<sup>[308]</sup> In addition, by using robots with different magnetization and friction, different swimming speeds resulting from the same magnetic field rotation frequency were applied to control two helical microrobots, which allows trajectories of the same shape but different size to be achieved.<sup>[309]</sup>

However, the methods mentioned above cannot control two microrobots to swim in the same direction at the same velocity because the robots are heterogeneous. Thus, to achieve fully individual control, recent work has found that planar motion can be realized by utilizing spatially varying gradients of the magnetic field with stationary electromagnetic coils.<sup>[310]</sup>

The frequency selectivity is also based on the principle of magnetic coupling resonance. microrobots can be driven independently if their structures possess different natural frequencies.<sup>[94]</sup> Such selectivity is shown in the top and bottom panels of Figure 12d). However, as illustrated in the middle panel of Figure 12d), when two microrobots experience the same control signal in the field source simultaneously, they will always be coupled in orientation, even though the robots can be sufficiently separated in frequency space. They differ only in the speed of movement. Thus, the simultaneous individual control cannot be stated to have been realized.<sup>[312]</sup> The feasibility of such control has been demonstrated theoretically,<sup>[313]</sup> but has not been practically tested.

Recent work has developed wavelength selectivity in the light-driven LCEs.<sup>[314]</sup> One manifestation of this concept uses the wavelength selectivity of plasmon resonance of nanometals.<sup>[315,316]</sup> Also, dye-doped LCEs<sup>[317]</sup> and LCEs doped with single-wall carbon nanotube (SWCNT) can achieve a similar function.<sup>[318]</sup> Because such materials are easy to assemble together, one mechanism can be fabricated with several independent parts that can only be actuated in a certain wavelength bandwidth. Hence, by applying different wavelengths sequentially, the mechanism can achieve complex multimode locomotion.<sup>[317]</sup>

Polarization selectivity is realized in the fabricating process, since the polarization of magnetic particles can be programmed by a variety of methods, such as electrodeposition of magnetic particles on lithographically printed microstructure,<sup>[319–321]</sup> lithographic patterning of magnetic nanoparticles,<sup>[85,322,323]</sup>

magnetic particles linked by deoxyribonucleic acid (DNA),<sup>[324]</sup> micro-assembly of magnetic components,<sup>[84,324,325]</sup> magnetic recording technology,<sup>[326]</sup> template-aided magnetizing,<sup>[327–329]</sup> 3D printing (DIW) of ferromagnetic domains,<sup>[84]</sup> and reorientation of magnetic particles by ultraviolet lithography.<sup>[214]</sup> When the magnetic is spatially programmed, each robot deforms to its specified shape, such as untethered gripper, centipede robot, zigzag spring, etc.,<sup>[214]</sup> after the magnetic field is applied. In this approach, the magnetic field does not need to be varied or modified; operation in a constant field from a permanent magnet is sufficient because the selective control is embodied in the structure of the robot.<sup>[84,214]</sup>

With the discovery of multi-stimuli materials and the development of multi-material composite processing, selectivity toward stimuli has become another research hotspot. For example, hydrogels are typical multi-stimuli materials that can be actuated by humidity, pH, light, temperature, and electricity.<sup>[51]</sup> The synergy of these stimuli can provide simple actuation mechanisms with multimodal locomotion ability.<sup>[52]</sup> In some cases, multi-stimuli materials can be used to modify the properties of the robot. For example, a pneumatic soft actuator combined with an shape memory polymer (SMP) skeleton uses air pressure to actuate and uses heat to modify the stiffness of the structure.<sup>[330]</sup> Similarly, Mishra et al. proposed a multi-material hydrogel actuator whose inner chamber is hydraulically driven, but the inner pressure is modulated by the temperature-dependent modulation of micropores.<sup>[331]</sup> These multifunctional materials provide new opportunities to create devices with unprecedented capabilities, but also require more sophisticated

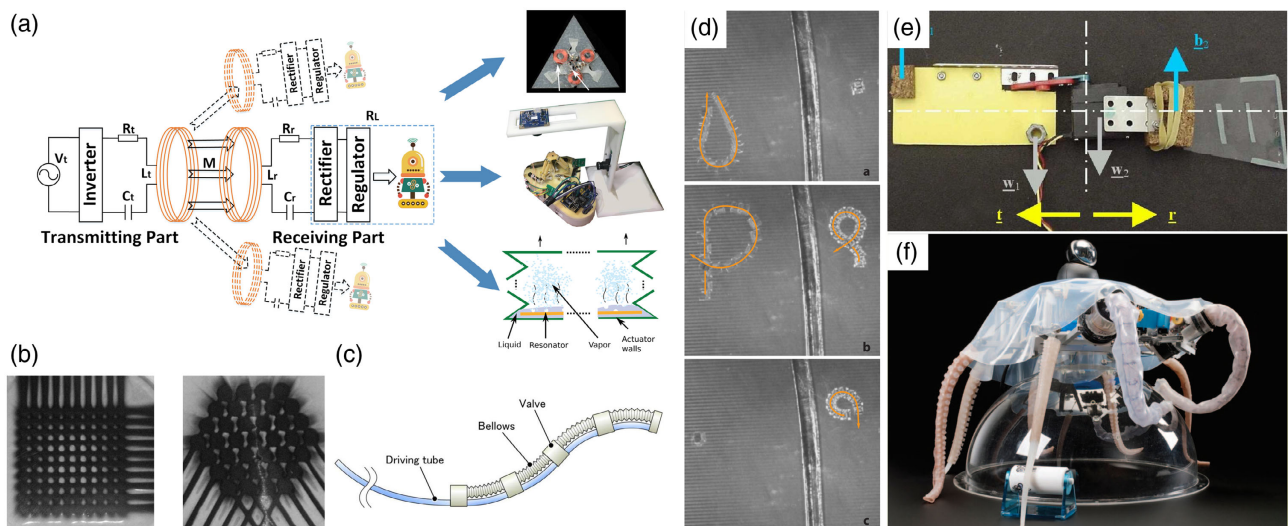


**Figure 12.** Underactuated soft robot with different control strategies. a) Multiplexing control based on WPT principle. Reproduced with permission.<sup>[240]</sup> Copyright 2021, ASME. Its applications in SMA actuators: Reproduced with permission.<sup>[104]</sup> Copyright 2017, AAAS. Motor: Reproduced with permission.<sup>[239]</sup> Copyright 2019, ASME. Pneumatic actuators: Reproduced with permission.<sup>[105]</sup> Copyright 2019, Wiley. b) Multiplexing control based on matrix addressing and its applications in tactile display with DEAs. Reproduced with permission.<sup>[354]</sup> Copyright 2009, SPIE. c) Multiplexing control based on bandpass value and its application in hydraulic soft robots. Reproduced with permission.<sup>[304]</sup> Copyright 2010, Springer. d) The selective control of magnetic micro-soft robots based on the frequency selectivity of magnetic coupling resonance. Reproduced with permission.<sup>[94]</sup> Copyright 2010, SAGE. e) Underactuated underwater swimming robot inspired by the morphological computation of fish structure. Reproduced with permission.<sup>[335]</sup> Copyright 2006, CLAWAR Association. f) Underactuated octopus-like eight-arm soft robot based on morphological computation. Reproduced with permission.<sup>[333]</sup> 2016, IEEE.

control systems. Model-based controllers that rely on knowledge of the robot structure and materials properties may be challenging to implement in these robots in which the materials' properties are intentionally variable.

There are several remaining general challenges in selective control. Selective control cannot become multiagent control since robots cannot be fully decoupled when using control signals simultaneously. Even though the robots can theoretically be separated sufficiently by frequency or time interval, current approaches can achieve independent control of only two–three devices, which is far from meeting the requirements for current multi-drive soft robots and swarm robots. In addition, one soft robot based on polarization selectivity can only achieve one pattern of motion since its selectivity is embodied in the fabrication process rather than the control system. Thus, increasing the number of actuators that can be independently controlled simultaneously is a key challenge in this field.

#### 5.4. Morphological computation based underactuated soft robot

“Morphological computation” is a concept that is built on observations of how the mechanical form of biological systems can provide the computational ability that reduces the complexity of the controller.<sup>[332,333]</sup> Often, tasks or subfunctions of the system can be performed autonomously without input from the controller, which is enabled by systems that contain dynamic coupling between elements or local feedback loops to accommodate environmental uncertainty. The concept is best summarized using examples, which we will draw from comprehensive reviews on the topic.<sup>[332,333]</sup> Insects are able to move very quickly over uneven terrain due to the structure of the legs, in which the joints are mechanically connected with compliant tissues that allow the leg to self-stabilize. This represents mechanical feedback that controls the mechanical functionality of the leg. Since it does not require input from the brain, the feedback can be very fast.

In many vertebrates, a central pattern generator (CPG) generates signals that control the movements of peripheral limbs.<sup>[333]</sup> In the example of swimming, the brain only needs to control the start signal and control the swimming pace, while the specific movements of the body are determined by local feedback loops formed by peripheral nerves throughout the body.<sup>[334]</sup> Inspired by the CPG, the legged robot whether soft or rigid with rhythmic movements can be controlled by fewer input signals than the quantity of the legs.<sup>[333]</sup> Similarly, a fish-like robot which is shown in Figure 12e) has only one motor as input, but has the ability to realize forward, turning, and vertical movement.<sup>[335]</sup>

An octopus controls the movement of its arms with only two parameters set by the brain, the trigger of the stiffening wave and the elbow angle.<sup>[336]</sup> However, due to local feedback from peripheral nerves and the mechanical coupling between segments of the arm, quite complex movements such as food delivering and fetching movement can be achieved.<sup>[333]</sup> Even though the octopus lacks a central representation of the arms, the peripheral nervous system shows an organization that fits the octopus' special embodiment.<sup>[337]</sup> The principles of morphological computation have been demonstrated in several octopus-inspired robots.<sup>[338–341]</sup>

To provide context for the role of morphological computation, Table 1 compares different forms of underactuated systems in terms of the actuator mechanisms, control strategies, methods of underactuation, input DOF, and output DOF. The pros and cons of each approach are emphasized.

Since morphological computing relies on the dynamic coupling between components, soft materials are an asset for morphological computing approaches. In addition, due to the infinite numbers of DOF in soft robots, morphological computing is a critical strategy for generating viable control strategies for sophisticated tasks in unstructured environments. However, the added DOF enabled by morphological computation is not the DOF defined in traditional robotics, but rather a new pattern of movement. Thus, it would be beneficial for this kind of

**Table 1.** The comparison of different forms of underactuated soft robot.

Actuator mechanisms	Control Form	Way of underactuation	Input DOF	Output DOF <sup>a)</sup>	Pros	Cons
SMA based on WPT <sup>[103,104,305]</sup>	Open-loop	Multiplexing	1	2–3	Universality, wireless	Switch control has no accuracy. The degree of multiplexing is low.
Motor based on WPT <sup>[239]</sup>	Closed-loop	Multiplexing	1	3	Universality, wireless, closed-loop control with a certain precision.	The degree of multiplexing is low.
DEAs <sup>[354]</sup>	Open-loop	Multiplexing	$2 \times n$	$n \times n$	High degree of multiplexing.	Only for sensor or display.
Hydraulic actuators <sup>[355]</sup>	Open-loop	Multiplexing	1	$n^b)$	No electrical component is required for a multiplexing control	Serial structure only
Magnetic micro-robot <sup>[94,310]</sup>	Autonomous	Selective control	1	2	Increase the motion complexity of the swarm microrobot.	Only for microrobot. The dimension of selectivity is limited yet.
Tendon driven by motor <sup>[340]</sup>	Open-loop	Morphological computation	1	4	Close to real-world environments and real-world tasks.	Different patterns of motion rather than DOF defined in robotics.
Wired motor <sup>[335]</sup>	Open-loop	Morphological computation	1	3	Close to real-world environments and real-world tasks.	Different patterns of motion rather than DOF defined in robotics.

<sup>a)</sup>Number of independent actuators; <sup>b)</sup>Based on the number of segments.

underactuation control method to be revisited from the perspective of robotics, such as DOF analysis and precision measurement, so that it can become more universal for all kinds of soft robots.

Strategies for implementing morphological computing in soft robots rely on new approaches for locally tailoring heterogeneous mechanical properties of materials<sup>[342]</sup> and integrating multiple functionalities. A typical hard robot might consist of a computer chip where the control algorithms are stored and executed, controllers such as an array of stepper motor amplifiers, stepper motors at each joint, and encoders that read out the position of each joint to provide feedback to the controller. The functions of decision-making (control algorithm), actuation, and sensing are all done by components that are physically and functionally distinct. In contrast, many biological systems are structured in such a way that sensing, actuation, and decision-making are distributed throughout the tissues and are interdependent. This co-location of sensing, information processing, and actuation enables multilevel embedded feedback loops that will play a role in the future development of morphological computing in soft robots. This paradigm of integrated fabrication of multifunctional systems has been under development for several years,<sup>[3,343]</sup> but is still in a nascent stage. Simple devices such as strain sensors and pneumatic actuators can be fabricated monolithically using multi-material 3D printing,<sup>[344,345]</sup> while more sophisticated devices such as transistors and memory are still fabricated separately and combined using wire bonding.<sup>[346]</sup> Approaches to recreate the full electromechanical functionality of the peripheral nervous system are under active development.<sup>[347]</sup>

### 5.5. Implementation of artificial intelligence

ML has been widely implemented in soft robots in the sensor and system characterization, kinematic and dynamic model, and controller.<sup>[275]</sup> Current ML algorithms often ignore the hysteresis and nonstationarity of soft materials or consider them as unmodeled noise. In addition, the well-known limitations of ML algorithms such as model bias, overfitting, and underfitting can lead to inaccurate predictions in soft robots.<sup>[275]</sup> As the field of robotics becomes more complex,<sup>[348]</sup> ML algorithms are becoming more widely adopted since it can be difficult to establish analytical models in these complex systems. As the number of coupled actuating segments increases, the control algorithms that would be required to specify the state of the system will become unmanageable using traditional approaches. Inspired by ML-based tomographic sensors,<sup>[271]</sup> programmable surfaces with dense actuator matrices could use ML algorithms to model the internal coupling between actuators.

AI approaches have been discussed at the software level (ML algorithms) for determining models. However, soft robots have physical characteristics that are intended to resemble biological organisms, and it is attractive to consider how AI can be introduced at the level of materials/hardware using approaches such as imitating the human nervous system. For example, artificial skin that senses multiple tactile signals (including force sensing for grip optimization, tensile strain sensing for proprioception, shear force sensing for object manipulation, and vibration

sensing for slip and texture detection) could provide soft robots with the same feeling and performance as human beings.<sup>[248,249]</sup> Organic artificial nerves<sup>[346]</sup> and neuromorphic transistors<sup>[349]</sup> can enable learning throughout the soft structure of the robot.

## 6. Conclusion

In this review, we introduced the control strategies and their implementation of soft robots from the perspective of the interplay between materials science and controls. The actuator mechanisms were classified by the energy source. Meanwhile, the control strategies were introduced based on the definition of control science with a biological interpretation. In the implementation of such control strategies, we focused on how different actuator mechanisms, algorithms, sensors, models, and hardware influence the implementation route of a soft robot system.

The interface between the controller and actuator changed rapidly with the development of materials science. Miniaturization and weight reduction have become important trends in the development of soft robots. These trends drive the development of control strategies to find methods to control underactuated systems while retaining the large DOF of the soft robot. This can be achieved by creating input signals that possess multiplexing characteristics, including TDM, SDM, and FDM. For a field energy source where there is no concept of an input signal, selective control can be realized by modulating the properties of the field or manufacturing devices with locally tailored magnetic properties. Based on inspiration from biology, the morphological computation can reduce the DOFs that need to be controlled directly. However, further work is necessary to increase the degree of underactuation and improve the reliability of control.

As the complexity of robots increases, ML is increasingly required to develop forward and inverse control algorithms. The rapid development of AI provides an alternative solution to take into account the nonlinear properties of novel materials and soft robots. ML algorithms developed for rigid robots provide inspiration for underactuated control systems for soft robots. Given that soft robots have similar mechanical properties to organisms, AI can be implemented at the hardware level in the form of artificial nerves and artificial synapses. A

Soft robots are an interdisciplinary field. It is not a simple extension of a traditional rigid robot. At present, every major breakthrough of soft robots integrates the research achievements in many fields, which requires the collaboration of scientists with different backgrounds. Similarly, the control strategy, one part of the soft robot, not only includes control structures and algorithms under a general point of view, but also is a comprehensive problem that should consider the implementation conditions of diverse actuator mechanisms, sensors, fabrication methods, and even application environments. With the development of material science, manufacturing technology, control science, artificial intelligence, soft robots may be created that can mimic or surpass the performance of natural organisms.

## Acknowledgements

We acknowledge the startup funds from Purdue University.

## Conflict of Interest

The authors declare no conflict of interest.

## Keywords

control strategies, soft actuators, soft robots, underactuated system

Received: September 8, 2021

Revised: January 22, 2022

Published online: February 22, 2022

- [1] P. Polygerinos, N. Correll, S. A. Morin, B. Mosadegh, C. D. Onal, K. Petersen, M. Cianchetti, M. T. Tolley, R. F. Shepherd, *Adv. Eng. Mater.* **2017**, *19*, 1700016.
- [2] C. Lee, M. Kim, Y. J. Kim, N. Hong, S. Ryu, H. J. Kim, S. Kim, *Int. J. Control Autom. Syst.* **2017**, *15*, 3.
- [3] T. Wallin, J. Pikul, R. Shepherd, *Nat. Rev. Mater.* **2018**, *3*, 84.
- [4] C. Walsh, *Nat. Rev. Mater.* **2018**, *3*, 78.
- [5] P. Polygerinos, Z. Wang, K. C. Galloway, R. J. Wood, C. J. Walsh, *Robot. Auton. Syst.* **2015**, *73*, 135.
- [6] E. W. Hawkes, L. H. Blumenschein, J. D. Greer, A. M. Okamura, *Sci. Robot.* **2017**, *2*, 8.
- [7] D. Rus, M. T. Tolley, *Nature* **2015**, *521*, 467.
- [8] S. I. Rich, R. J. Wood, C. Majidi, *Nat. Electron.* **2018**, *1*, 102.
- [9] N. El-Atab, R. B. Mishra, F. Al-Modaf, L. Joharji, A. A. Alsharif, H. Alamoudi, M. Diaz, N. Qaiser, M. M. Hussain, *Adv. Intell. Syst.* **2020**, *2*, 2000128.
- [10] S. M. Mirvakili, I. W. Hunter, *Adv. Mater.* **2018**, *30*, 1704407.
- [11] J. M. McCracken, B. R. Donovan, T. J. White, *Adv. Mater.* **2020**, *32*, 1906564.
- [12] D. Chen, Q. Pei, *Chem. Rev.* **2017**, *117*, 11239.
- [13] C. Laschi, B. Mazzolai, M. Cianchetti, *Sci. Robot.* **2016**, *1*, eaah3690.
- [14] T. George Thuruthel, Y. Ansari, E. Falotico, C. Laschi, *Soft Robot.* **2018**, *5*, 149.
- [15] S. Hashemi, D. Bentivegna, W. Durfee, *Soft Robot.* **2020**, *8*, 387.
- [16] R. K. Katzschnmann, A. D. Marchese, D. Rus, in *Experimental Robotics*, Springer, Cham **2016**, pp. 405–420.
- [17] A. D. Marchese, D. Rus, *Int. J. Robot. Res.* **2016**, *35*, 840.
- [18] E. Brown, N. Rodenberg, J. Amend, A. Mozeika, E. Steltz, M. R. Zakin, H. Lipson, H. M. Jaeger, *Proc. Natl. Acad. Sci. U.S.A.* **2010**, *107*, 18809.
- [19] J. R. Amend, E. Brown, N. Rodenberg, H. M. Jaeger, H. Lipson, *IEEE Trans. Robot.* **2012**, *28*, 341.
- [20] M. A. Robertson, J. Paik, *Sci. Robot.* **2017**, *2*, 9.
- [21] H. Habibi, P. Land, M. J. Ball, D. A. Troncoso, D. T. Branson III, *J. Manuf. Process* **2018**, *32*, 241.
- [22] Z. Zhang, G. Chen, H. Wu, L. Kong, H. Wang, *IEEE Robot. Autom. Lett.* **2020**, *5*, 3564.
- [23] L. Paez, G. Agarwal, J. Paik, *Soft Robot.* **2016**, *3*, 109.
- [24] S. Li, D. M. Vogt, D. Rus, R. J. Wood, *Proc. Natl. Acad. Sci. U.S.A.* **2017**, *114*, 13132.
- [25] J. T. Overvelde, T. A. De Jong, Y. Shevchenko, S. A. Becerra, G. M. Whitesides, J. C. Weaver, C. Hoberman, K. Bertoldi, *Nat. Commun.* **2016**, *7*, 1.
- [26] M. Adami, A. Seibel, in *Actuators*, Vol. 8, Multidisciplinary Digital Publishing Institute, **2019**, *8*, p. 2.
- [27] M. Wehner, M. T. Tolley, Y. Mengüç, Y.-L. Park, A. Mozeika, Y. Ding, C. Onal, R. F. Shepherd, G. M. Whitesides, R. J. Wood, *Soft Robot.* **2014**, *1*, 263.
- [28] C. D. Onal, X. Chen, G. M. Whitesides, D. Rus, in *Robotics Research*, Springer, **2017**, pp. 525–540.
- [29] F. Vitale, D. Accoto, L. Turchetti, S. Indini, M. C. Annesini, E. Guglielmelli, in *2010 IEEE ICRA*, IEEE, Piscataway, NJ **2010**, pp. 2197–2202.
- [30] M. Goldfarb, E. J. Barth, M. A. Gogola, J. A. Wehrmeyer, *IEEE ASME Trans. Mechatron.* **2003**, *8*, 254.
- [31] I. A. Salem, M. El-Maazawi, A. B. Zaki, *Int. J. Chem. Kinet.* **2000**, *32*, 643.
- [32] A. Chortos, J. Mao, J. Mueller, E. Hajiesmaili, J. A. Lewis, D. R. Clarke, *Adv. Funct. Mater.* **2021**, *31*, 2010643.
- [33] U. Gupta, L. Qin, Y. Wang, H. Godaba, J. Zhu, *Smart Mater. Struct.* **2019**, *28*, 103002.
- [34] Y. Li, I. Oh, J. Chen, H. Zhang, Y. Hu, *Int. J. Solids Struct.* **2018**, *152*, 28.
- [35] S. Shian, K. Bertoldi, D. R. Clarke, *Adv. Mater.* **2015**, *27*, 6814.
- [36] T. Wang, J. Zhang, J. Hong, M. Y. Wang, *Soft Robot.* **2017**, *4*, 61.
- [37] X. Ji, X. Liu, V. Cacucciolo, M. Imboden, Y. Civet, A. El Haitami, S. Cantin, Y. Perriard, H. Shea, *Sci. Robot.* **2019**, *4*, 37.
- [38] E.-F. M. Henke, S. Schlatter, I. A. Anderson, *Soft Robot.* **2017**, *4*, 353.
- [39] A. Chortos, E. Hajiesmaili, J. Morales, D. R. Clarke, J. A. Lewis, *Adv. Funct. Mater.* **2020**, *30*, 1907375.
- [40] G. Haghiashtiani, E. Habtour, S. Park, F. Gardea, M. McAlpine, *Extreme Mech. Lett.* **2018**, *21*, 1.
- [41] M. R. O'Neill, E. Acome, S. Bakarich, S. K. Mitchell, J. Timko, C. Keplinger, R. F. Shepherd, *Adv. Funct. Mater.* **2020**, *30*, 2005244.
- [42] S. Schlatter, G. Grasso, S. Rosset, H. Shea, *Adv. Intell. Syst.* **2020**, *2*, 2000136.
- [43] Y.-Y. Chiu, W.-Y. Lin, H.-Y. Wang, S.-B. Huang, M.-H. Wu, *Sens. Actuator A Phys.* **2013**, *189*, 328.
- [44] K.-I. Park, C. K. Jeong, N. K. Kim, K. J. Lee, *Nano Converg.* **2016**, *3*, 1.
- [45] Y. Qi, N. T. Jafferis, K. Lyons Jr, C. M. Lee, H. Ahmad, M. C. McAlpine, *Nano Lett.* **2010**, *10*, 524.
- [46] K. J. Kim, S. Tadokoro, *Artif. Muscles Sens.* **2007**, *23*, 291.
- [47] Y. Bar-Cohen, in *Smart Structure and Materials 2004: EAPAD*, Vol. 5385, International Society for Optics and Photonics, **2004**, pp. 10–16.
- [48] Y. Nakabo, T. Mukai, K. Asaka, in *IEEE 2005 ICRA*, IEEE, Piscataway, NJ **2005**, pp. 4315–4320.
- [49] S. Guo, T. Fukuda, K. Asaka, *IEEE ASME Trans. Mechatron.* **2003**, *8*, 136.
- [50] E. N. Gama Melo, O. F. Aviles Sanchez, D. Amaya Hurtado, *Inginería y Desarrollo* **2014**, *32*, 279.
- [51] H. Zhu, B. Xu, Y. Wang, X. Pan, Z. Qu, Y. Mei, *Sci. Robot.* **2021**, *6*, 53.
- [52] C. Li, G. C. Lau, H. Yuan, A. Aggarwal, V. L. Dominguez, S. Liu, H. Sai, L. C. Palmer, N. A. Sather, T. J. Pearson, D. E. Freedman, P. K. Amiri, M. O. de la Cruz, S. I. Stupp, *Sci. Robot.* **2020**, *5*, 49.
- [53] A. Tonazzini, A. Sadeghi, B. Mazzolai, *Soft Robot.* **2016**, *3*, 34.
- [54] C. Majidi, R. J. Wood, *Appl. Phys. Lett.* **2010**, *97*, 164104.
- [55] A. Sadeghi, L. Beccai, B. Mazzolai, in *2012 IEEE/RSJ IROS*, IEEE, Piscataway, NJ **2012**, pp. 4237–4242.
- [56] T. Noritsugu, Y. Tsuji, *Trans. Soc. Instrum. Control Eng.* **2001**, *37*, 590.
- [57] J. Shintake, S. Rosset, B. Schubert, D. Floreano, H. Shea, *Adv. Mater.* **2016**, *28*, 231.
- [58] G. Gu, J. Zou, R. Zhao, X. Zhao, X. Zhu, *Sci. Robot.* **2018**, *3*, 25.
- [59] J. Guo, K. Elgeneidy, C. Xiang, N. Lohse, L. Justham, J. Rossiter, *Smart Mater. Struct.* **2018**, *27*, 055006.
- [60] S. Diller, C. Majidi, S. H. Collins, in *2016 IEEE ICRA*, IEEE, Piscataway, NJ **2016**, pp. 682.
- [61] J. Germann, B. Schubert, D. Floreano, in *2014 IEEE/RSJ IROS*, IEEE, Piscataway, NJ **2014**, pp. 3933–3938.
- [62] A. Bajo, R. E. Goldman, N. Simaan, in *2011 IEEE Int. Conf. on Robotics and Automation*, IEEE, Piscataway, NJ **2011**, pp. 2905–2912.

- [63] H. Su, D. C. Cardona, W. Shang, A. Camilo, G. A. Cole, D. C. Rucker, R. J. Webster, G. S. Fischer, in *2012 IEEE ICRA*, IEEE, Piscataway, NJ **2012**, pp. 1939–1945.
- [64] X. Huang, K. Kumar, M. K. Jawed, A. M. Nasab, Z. Ye, W. Shan, C. Majidi, *Sci. Robot.* **2018**, 3, eaau7557.
- [65] H. Rodrigue, W. Wang, D.-R. Kim, S.-H. Ahn, *Compos. Struct.* **2017**, 176, 398.
- [66] E. Sachyani Kenneth, G. Scalet, M. Layani, G. Tibi, A. Degani, F. Auricchio, S. Magdassi, *Soft Robot.* **2020**, 7, 123.
- [67] S. Yao, J. Cui, Z. Cui, Y. Zhu, *Nanoscale* **2017**, 9, 3797.
- [68] Y. Tian, Y.-T. Li, H. Tian, Y. Yang, T.-L. Ren, *Soft Robot.* **2020**.
- [69] J.-B. Chossat, D. K. Chen, Y.-L. Park, P. B. Shull, *IEEE Trans. Haptics* **2019**, 12, 521.
- [70] M. Kanik, S. Orguc, G. Varnavides, J. Kim, T. Benavides, D. Gonzalez, T. Akintilo, C. C. Tasan, A. P. Chandrasekaran, Y. Fink, P. Anikeeva, *Science* **2019**, 365, 145.
- [71] D. Gao, M.-F. Lin, J. Xiong, S. Li, S. N. Lou, Y. Liu, J.-H. Ciou, X. Zhou, P. S. Lee, *Nanoscale Horiz.* **2020**, 5, 730.
- [72] L. Dong, Y. Zhao, *Mater. Chem. Front.* **2018**, 2, 1932.
- [73] X. Pang, J.-a. Lv, C. Zhu, L. Qin, Y. Yu, *Adv. Mater.* **2019**, 31, 1904224.
- [74] S. Huang, Y. Shen, H. K. Bisoyi, Y. Tao, Z. Liu, M. Wang, H. Yang, Q. Li, *J. Am. Chem. Soc.* **2021**, 143, 12543.
- [75] B. Han, Y.-L. Zhang, Q.-D. Chen, H.-B. Sun, *Adv. Funct. Mater.* **2018**, 28, 1802235.
- [76] W. Hu, K. S. Ishii, A. T. Ohta, *Appl. Phys. Lett.* **2011**, 99, 094103.
- [77] W. Hu, K. S. Ishii, Q. Fan, A. T. Ohta, *Lab Chip* **2012**, 12, 3821.
- [78] B. J. Park, F. F. Fang, H. J. Choi, *Soft Matter* **2010**, 6, 5246.
- [79] M. Zrnyi, D. Szabó, H.-G. Kilian, *Polym. Gels Netw.* **1998**, 6, 441.
- [80] J. Kim, S. E. Chung, S.-E. Choi, H. Lee, J. Kim, S. Kwon, *Nat. Mater.* **2011**, 10, 747.
- [81] K. B. Yesin, K. Vollmers, B. J. Nelson, *Int. J. Rob. Res.* **2006**, 25, 527.
- [82] B. Yigit, Y. Alapan, M. Sitti, *Adv. Sci.* **2019**, 6, 1801837.
- [83] E. B. Joyee, Y. Pan, *Soft Robot.* **2019**, 6, 333.
- [84] Y. Kim, H. Yuk, R. Zhao, S. A. Chester, X. Zhao, *Nature* **2018**, 558, 274.
- [85] H.-W. Huang, M. S. Sakar, A. J. Petruska, S. Pané, B. J. Nelson, *Nat. Commun.* **2016**, 7, 1.
- [86] J. A.-C. Liu, J. H. Gillen, S. R. Mishra, B. A. Evans, J. B. Tracy, *Sci. Adv.* **2019**, 5, eaaw2897.
- [87] E. Diller, M. Sitti, *Adv. Funct. Mater.* **2014**, 24, 4397.
- [88] O. Erin, D. Antonelli, M. E. Tiriyaki, M. Sitti, in *2020 IEEE ICRA*, IEEE, Piscataway, NJ **2020**, pp. 6551–6557.
- [89] S. Jeon, G. Jang, H. Choi, S. Park, *IEEE Trans. Magn.* **2010**, 46, 1943.
- [90] S. Jeon, G. Jang, H. Choi, S. Park, J. Park, *J. Appl. Phys.* **2012**, 111, 07E702.
- [91] S. Floyd, C. Pawashe, M. Sitti, in *2008 IEEE ICRA*, IEEE, Piscataway, NJ **2008**, pp. 419–424.
- [92] Z. Nagy, B. J. Nelson, *IEEE Trans. Robot.* **2012**, 28, 787.
- [93] M. P. Kummer, J. J. Abbott, B. E. Kratochvil, R. Borer, A. Sengul, B. J. Nelson, *IEEE Trans. Robot.* **2010**, 26, 1006.
- [94] D. R. Frutiger, K. Vollmers, B. E. Kratochvil, B. J. Nelson, *Int. J. Rob. Res.* **2010**, 29, 613.
- [95] K. Xu, G. Liu, in *ICIRA 2013*, Springer, Busan, South Korea **2013**, pp. 143–154.
- [96] H.-W. Tung, M. Maffioli, D. R. Frutiger, K. M. Sivaraman, S. Pané, B. J. Nelson, *IEEE Trans. Robot.* **2013**, 30, 26.
- [97] J. C. Kuo, H. W. Huang, S. W. Tung, Y. J. Yang, *Sens. Actuators A Phys.* **2014**, 211, 121.
- [98] J. M. Jani, M. Leary, A. Subic, M. A. Gibson, *Mater. Des.* **2014**, 56, 1078.
- [99] D. Kim, K. Hwang, J. Park, H. H. Park, S. Ahn, in *2016 IEEE CEFC*, IEEE, Piscataway, NJ **2016**, pp. 1.
- [100] A. Kurs, A. Karalis, R. Moffatt, J. D. Joannopoulos, P. Fisher, M. Soljačić, *Science* **2007**, 317, 83.
- [101] S. Ho, J. Wang, W. Fu, M. Sun, *IEEE Trans. Magn.* **2011**, 47, 1522.
- [102] B. L. Cannon, J. F. Hoburg, D. D. Stancil, S. C. Goldstein, *IEEE Trans. Power Electron.* **2009**, 24, 1819.
- [103] C. Mc Caffrey, T. Umedachi, W. Jiang, T. Sasatani, Y. Narusue, R. Niyyama, Y. Kawahara, *Soft Robot.* **2020**, 7, 700.
- [104] M. Boyvat, J.-S. Koh, R. J. Wood, *Sci. Robot.* **2017**, 2, 8.
- [105] M. Boyvat, D. M. Vogt, R. J. Wood, *Adv. Mater. Technol.* **2019**, 4, 1800381.
- [106] C. T. Nguyen, H. Phung, H. Jung, U. Kim, T. D. Nguyen, J. Park, H. Moon, J. C. Koo, H. R. Choi, in *2015 IEEE ICRA*, IEEE, Piscataway, NJ **2015**, pp. 4484–4489.
- [107] P. Polygerinos, Z. Wang, J. T. Overvelde, K. C. Galloway, R. J. Wood, K. Bertoldi, C. J. Walsh, *IEEE Trans. Robot.* **2015**, 31, 778.
- [108] D. Drotman, S. Jadhav, M. Karimi, P. Dezonia, M. T. Tolley, in *2017 IEEE ICRA*, IEEE, Piscataway, NJ **2017**, pp. 5532–5538.
- [109] F. Ilievski, A. D. Mazzeo, R. F. Shepherd, X. Chen, G. M. Whitesides, *Angew. Chem., Int. Ed.* **2011**, 123, 1930.
- [110] B. Gorissen, D. Melancon, N. Vasios, M. Torbati, K. Bertoldi, *Sci. Robot.* **2020**, 5, 42.
- [111] I. A. Gravagne, C. D. Rahn, I. D. Walker, *IEEE ASME Trans. Mechatron.* **2003**, 8, 299.
- [112] G. S. Chirikjian, *Adv. Robot.* **1994**, 9, 217.
- [113] Y. Yekutieli, R. Sagiv-Zohar, R. Aharonov, Y. Engel, B. Hochner, T. Flash, *J. Neurophysiol.* **2005**, 94, 1443.
- [114] E. Tatlicioğlu, I. D. Walker, D. M. Dawson, in *IEEE 2007 ICRA*, IEEE, Piscataway, NJ **2007**, pp. 1357–1362.
- [115] A. D. Marchese, R. Tedrake, D. Rus, *Int. J. Rob. Res.* **2016**, 35, 1000.
- [116] R. K. Katzschnmann, C. Della Santina, Y. Toshimitsu, A. Bicchi, D. Rus, in *2019 2nd IEEE RoboSoft*, IEEE, Piscataway, NJ **2019**, pp. 454–461.
- [117] C. Della Santina, R. K. Katzschnmann, A. Biechi, D. Rus, in *2018 IEEE RoboSoft*, IEEE, Piscataway, NJ **2018**, pp. 46–53.
- [118] F. Branz, A. Francesconi, *Smart Mater. Struct.* **2016**, 25, 095040.
- [119] C. M. Best, M. T. Gillespie, P. Hyatt, L. Rupert, V. Sherrod, M. D. Killpack, *IEEE Robot. Autom. Mag.* **2016**, 23, 75.
- [120] Z. Q. Tang, H. L. Heung, K. Y. Tong, Z. Li, *Int. J. Rob. Res.* **2019**, 0278364919873379.
- [121] R. B. Gorbet, R. A. Russell, *Robotica* **1995**, 13, 423.
- [122] N. R. Sinatra, C. B. Teeple, D. M. Vogt, K. K. Parker, D. F. Gruber, R. J. Wood, *Sci. Robot.* **2019**, 4, 33.
- [123] C. Della Santina, R. K. Katzschnmann, A. Bicchi, D. Rus, *Int. J. Rob. Res.* **2020**, 39, 490.
- [124] J. Zhang, B. Wang, C. Zhang, Y. Xiao, M. Y. Wang, *Front. Neurorobot.* **2019**, 13, 7.
- [125] A. Bajo, N. Simaan, *Int. J. Rob. Res.* **2016**, 35, 422.
- [126] F. Ongaro, S. Scheggi, C. Yoon, F. Van den Brink, S. H. Oh, D. H. Gracias, S. Misra, *J. Micro-Bio Robot.* **2017**, 12, 45.
- [127] L. Chen, W. Chen, Y. Xue, J.-W. Wong, Y. Liang, M. Zhang, X. Chen, X. Cao, Z. Zhang, T. Li, *Extreme Mech. Lett.* **2019**, 27, 27.
- [128] B. Zhang, Y. Fan, P. Yang, T. Cao, H. Liao, *Soft Robot.* **2019**, 6, 399.
- [129] T. A. Gisby, B. M. O'Brien, I. A. Anderson, *Appl. Phys. Lett.* **2013**, 102, 193703.
- [130] G. Rizzello, P. Serafino, D. Naso, S. Seelecke, *IEEE Trans. Robot.* **2019**, 36, 174.
- [131] K. Ly, N. Kellaris, D. McMorris, B. K. Johnson, E. Acome, V. Sundaram, M. Naris, J. S. Humbert, M. E. Rentschler, C. Keplinger, N. Correll, *Soft Robot.* **2020**, 8, 673.
- [132] A. Kotikian, J. M. Morales, A. Lu, J. Mueller, Z. S. Davidson, J. W. Boley, J. A. Lewis, *Adv. Mater.* **2021**, 2101814.
- [133] R. A. Bilodeau, E. L. White, R. K. Kramer, in *2015 IEEE/RSJ IROS*, IEEE, Piscataway, NJ **2015**, pp. 2324–2329.

- [134] E. H. Skorina, M. Luo, S. Ozel, F. Chen, W. Tao, C. D. Onal, in 2015 *IEEE ICRA*, IEEE, Piscataway, NJ **2015**, pp. 2544–2549.
- [135] M. Turkseven, J. Ueda, in 2016 *IEEE ICRA*, IEEE, Piscataway, NJ, pp. 1160–1165.
- [136] T. Wang, J. Zhang, J. Hong, M. Y. Wang, *Soft Robot.* **2017**, *4*, 61.
- [137] Y. Chen, H. Zhao, J. Mao, P. Chirarattananon, E. F. Helbling, N.-s. P. Hyun, D. R. Clarke, R. J. Wood, *Nature* **2019**, *575*, 324.
- [138] X. Ji, X. Liu, V. Cacucciolo, M. Imboden, Y. Civet, A. El Haitami, S. Cantin, Y. Perriard, H. Shea, *Sci. Robot.* **2019**, *4*, 37.
- [139] P. Rothermund, A. Ainla, L. Belding, D. J. Preston, S. Kurihara, Z. Suo, G. M. Whitesides, *Sci. Robot.* **2018**, *3*, 16.
- [140] C. D. Onal, D. Rus, *Bioinspir. Biomim.* **2013**, *8*, 026003.
- [141] F. Connolly, C. J. Walsh, K. Bertoldi, *Proc. Natl. Acad. Sci. U.S.A.* **2017**, *114*, 51.
- [142] M. C. Yip, D. B. Camarillo, *IEEE Robot. Autom. Lett.* **2016**, *1*, 844.
- [143] L. Li, J. Li, L. Qin, J. Cao, M. S. Kankanhalli, J. Zhu, *IEEE Robot. Autom. Lett.* **2019**, *4*, 2094.
- [144] S. Han, T. Kim, D. Kim, Y.-L. Park, S. Jo, *IEEE Robot. Autom. Lett.* **2018**, *3*, 873.
- [145] T. G. Thuruthel, B. Shih, C. Laschi, M. T. Tolley, *Sci. Robot.* **2019**, *4*, 26.
- [146] H. Jiang, Z. Wang, X. Liu, X. Chen, Y. Jin, X. You, X. Chen, in 2017 *IEEE ICRA*, IEEE, Piscataway, NJ **2017**, pp. 6127–6133.
- [147] T. G. Thuruthel, E. Falotico, F. Renda, C. Laschi, *Bioinspir. Biomim.* **2017**, *12*, 066003.
- [148] M. Giorelli, F. Renda, M. Calisti, A. Arienti, G. Ferri, C. Laschi, *IEEE Trans. Robot.* **2015**, *31*, 823.
- [149] S. K. Pradhan, B. Subudhi, *IEEE Trans. Autom. Sci. Eng.* **2012**, *9*, 237.
- [150] L. Tian, J. Wang, Z. Mao, *IEEE Trans. Syst. Man Cybern. Syst.* **2004**, *34*, 1541.
- [151] T. G. Thuruthel, E. Falotico, F. Renda, C. Laschi, *IEEE Trans. Robot.* **2018**, *35*, 124.
- [152] T. G. Thuruthel, E. Falotico, F. Renda, C. Laschi, *Bioinspir. Biomim.* **2017**, *12*, 066003.
- [153] D. Braganza, D. M. Dawson, I. D. Walker, N. Nath, *IEEE Trans. Robot.* **2007**, *23*, 1270.
- [154] Y. Engel, P. Szabo, D. Volkinshtein, *Adv. Neural Inf. Process. Syst.* **2005**, *18*, 347.
- [155] G. Fang, X. Wang, K. Wang, K.-H. Lee, J. D. Ho, H.-C. Fu, D. K. C. Fu, K.-W. Kwok, *IEEE Robot. Autom. Lett.* **2019**, *4*, 1194.
- [156] X. Wang, G. Fang, K. Wang, X. Xie, K.-H. Lee, J. D. Ho, W. L. Tang, J. Lam, K.-W. Kwok, *IEEE Robot. Autom. Lett.* **2020**, *5*, 2161.
- [157] H. Kim, U. K. Cheang, L. W. Rogowski, M. J. Kim, *J. Micro-Bio Robot.* **2018**, *14*, 41.
- [158] S. Mintchev, D. Zappetti, J. Willermin, D. Floreano, in 2018 *IEEE ICRA*, IEEE, Piscataway, NJ **2018**, pp. 7492–7497.
- [159] O. Goury, C. Duriez, *IEEE Trans. Robot.* **2018**, *34*, 1565.
- [160] C. C. Foo, Z.-Q. Zhang, *Int. J. Appl. Mech.* **2015**, *7*, 1550069.
- [161] E. Coevoet, A. Escande, C. Duriez, in 2019 2nd *IEEE RoboSoft*, IEEE, Piscataway, NJ **2019**, pp. 739–745.
- [162] J. M. Bern, P. Banzet, R. Poranne, S. Coros, *Robot.: Sci. Syst.* **2019**.
- [163] B. O'Brien, E. Calius, S. Xie, I. Anderson, in *Smart Struct. Mater. 2008: EAPAD*, Vol. 6927, International Society for Optics and Photonics, **2008**, p. 69270T.
- [164] L. Jin, A. Takei, J. W. Hutchinson, *J. Mech. Phys. Solids* **2015**, *81*, 22.
- [165] H. S. Park, Z. Suo, J. Zhou, P. A. Klein, *Int. J. Solids Struct.* **2012**, *49*, 2187.
- [166] F. Simone, P. Linnebach, G. Rizzello, S. Seelecke, *Smart Mater. Struct.* **2018**, *27*, 065001.
- [167] K. Jia, M. Wang, T. Lu, T. Wang, *Int. J. Mech. Sci.* **2019**, *159*, 441.
- [168] Y. Zhang, Y. Peng, Z. Sun, H. Yu, *IEEE Trans. Ind. Electron.* **2018**, *66*, 5374.
- [169] G. Mao, W. Hong, M. Kaltenbrunner, S. Qu, *J. Appl. Mech.* **2021**, *88*, 101007.
- [170] E. Garnell, C. Rouby, O. Doaré, *Smart Mater. Struct.* **2021**, *30*, 025031.
- [171] R. Neugebauer, A. Bucht, K. Pagel, J. Jung, in *Industrial and Commercial Applications of Smart Structures Technologies 2010*, Vol. 7645, International Society for Optics and Photonics, **2010**, p. 76450J.
- [172] T. Merzouki, A. Duval, T. B. Zineb, *Simul. Model Pract. Theory* **2012**, *27*, 112.
- [173] X. Tang, Y. Liu, K. Li, W. Chen, J. Zhao, *Mater. Res. Express* **2018**, *5*, 015701.
- [174] C. Wu, Y. Xiang, S. Qu, Y. Song, Q. Zheng, *J. Phys. D* **2020**, *53*, 235402.
- [175] E. B. Joyee, Y. Pan, *Soft Robot.* **2019**, *6*, 333.
- [176] E. B. Joyee, Y. Pan, *J. Manuf. Process* **2020**, *56*, 1178.
- [177] G. Mao, M. Drack, M. Karami-Mosammam, D. Wirthl, T. Stockinger, R. Schwödäuer, M. Kaltenbrunner, *Sci. Adv.* **2020**, *6*, eabc0251.
- [178] C. Duriez, in 2013 *IEEE ICRA*, IEEE, Piscataway, NJ **2013**, pp. 3982–3987.
- [179] F. Largilliere, V. Verona, E. Coevoet, M. Sanz-Lopez, J. Dequidt, C. Duriez, in 2015 *IEEE ICRA*, IEEE, Piscataway, NJ **2015**, pp. 2550–2555.
- [180] T. Beda, *J. Polym. Sci. B Polym. Phys.* **2007**, *45*, 1713.
- [181] Z. Liu, F. Wang, S. Liu, Y. Tian, D. Zhang, *IEEE ASME Trans. Mechatron.* **2020**, *26*, 2195.
- [182] Y. Li, I. Oh, J. Chen, H. Zhang, Y. Hu, *Int. J. Solids Struct.* **2018**, *152*, 28.
- [183] C.-P. Chou, B. Hannaford, *IEEE Trans. Robot. Autom.* **1996**, *12*, 90.
- [184] P. Paoletti, G. Jones, L. Mahadevan, *J. R. Soc. Interface* **2017**, *14*, 20160867.
- [185] R. E. Pelrine, R. D. Kornbluh, J. P. Joseph, *Sens. Actuator A Phys.* **1998**, *64*, 77.
- [186] M. Wissler, E. Mazza, *Sens. Actuator A Phys.* **2007**, *138*, 384.
- [187] Z. Suo, *Acta Mechanica Solida Sinica* **2010**, *23*, 549.
- [188] U. Gupta, Y. Wang, H. Ren, J. Zhu, *IEEE ASME Trans. Mechatron.* **2018**, *24*, 25.
- [189] W. J. Yoon, P. G. Reinhard, E. J. Seibel, *Sens. Actuator A Phys.* **2007**, *133*, 506.
- [190] J. Madden, in *Electroactive Polymers for Robotic Applications*, Springer, **2007**, pp. 121–152.
- [191] F. Karami, Y. Tadesse, *Smart Mater. Struct.* **2017**, *26*, 125010.
- [192] F. Kong, Y. Zhu, C. Yang, H. Jin, J. Zhao, H. Cai, *IEEE Trans. Ind. Electron.* **2020**, *68*, 5078.
- [193] H. Niu, R. Feng, Y. Xie, B. Jiang, Y. Sheng, Y. Yu, H. Baoyin, X. Zeng, *Soft Robot.* **2020**, *8*, 507.
- [194] I. S. Godage, R. Wirz, I. D. Walker, R. J. Webster III, *Soft Robot.* **2015**, *2*, 96.
- [195] S. H. Sadati, S. E. Naghibi, A. Shiva, I. D. Walker, K. Althoefer, T. Nanayakkara, in *Annual Conf. Towards Autonomous Robotic Systems*, Springer, **2017**, pp. 686–702.
- [196] R. J. Webster III, B. A. Jones, *Int. J. Rob. Res.* **2010**, *29*, 1661.
- [197] G. Runge, A. Raatz, *CIRP Ann. Manuf. Technol.* **2017**, *66*, 9.
- [198] V. Falkenhahn, A. Hildebrandt, R. Neumann, O. Sawodny, in 2015 *IEEE ICRA*, IEEE, Piscataway, NJ **2015**, pp. 762–767.
- [199] L. Weerakoon, N. Chopra, in 2020 *IEEE ACC*, IEEE, Piscataway, NJ **2020**, pp. 2124–2129.
- [200] T. Mahl, A. E. Mayer, A. Hildebrandt, O. Sawodny, in 2013 *IEEE ACC*, IEEE, Piscataway, NJ **2013**, pp. 4945–4950.
- [201] D. Trivedi, A. Lotfi, C. D. Rahn, *IEEE Trans. Robot.* **2008**, *24*, 773.
- [202] M. Bergou, M. Wardetzky, S. Robinson, B. Audoly, E. Grinshpan, in *ACM SIGGRAPH 2008 papers*, **2008**, pp. 1–12.

- [203] M. Gazzola, L. Dudte, A. McCormick, L. Mahadevan, *R. Soc. Open Sci.* **2018**, *5*, 171628.
- [204] M. Dehghani, S. A. A. Moosavian, in *2011 IEEE/ASME AIM*, IEEE, Piscataway, NJ **2011**, pp. 966–971.
- [205] H.-S. Chang, U. Halder, C.-H. Shih, A. Tekinalp, T. Parthasarathy, E. Gribkova, G. Chowdhary, R. Gillette, M. Gazzola, P. G. Mehta, in *2020 59th IEEE CDC*, IEEE, Piscataway, NJ **2020**, pp. 3913–3920.
- [206] F. Renda, M. Giorelli, M. Calisti, M. Cianchetti, C. Laschi, *IEEE Trans. Robot.* **2014**, *30*, 1109.
- [207] D. Trivedi, A. Lotfi, C. D. Rahn, in *2007 IEEE/RSJ IROS*, IEEE, Piscataway, NJ **2007**, pp. 1497–1502.
- [208] X. Zhang, F. K. Chan, T. Parthasarathy, M. Gazzola, *Nat. Commun.* **2019**, *10*, 1.
- [209] S. H. Sadati, S. E. Naghibi, I. D. Walker, K. Althoefer, T. Nanayakkara, *IEEE Robot. Autom. Lett.* **2017**, *3*, 328.
- [210] G. S. Chirikjian, J. W. Burdick, *IEEE Trans. Robot. Autom.* **1995**, *11*, 781.
- [211] T. Zheng, D. T. Branson, R. Kang, M. Cianchetti, E. Guglielmino, M. Follador, G. A. Medrano-Cerda, I. S. Godage, D. G. Caldwell, in *2012 IEEE ICRA*, IEEE, Piscataway, NJ **2012**, pp. 5289–5294.
- [212] Y. Kim, H. Yuk, R. Zhao, S. A. Chester, X. Zhao, *Nature* **2018**, *558*, 274.
- [213] Y. Kim, G. A. Parada, S. Liu, X. Zhao, *Sci. Robot.* **2019**, *4*, 33.
- [214] T. Xu, J. Zhang, M. Salehizadeh, O. Onaizah, E. Diller, *Sci. Robot.* **2019**, *4*, 29.
- [215] L. Zheng, L.-g. Chen, H.-b. Huang, X.-p. Li, L.-l. Zhang, *Microsyst. Technol.* **2016**, *22*, 2371.
- [216] H. Choi, J. Choi, G. Jang, J.-o. Park, S. Park, *Smart Mater. Struct.* **2009**, *18*, 055007.
- [217] C. Yu, J. Kim, H. Choi, J. Choi, S. Jeong, K. Cha, J.-o. Park, S. Park, *Sens. Actuator A Phys.* **2010**, *161*, 297.
- [218] Y. Wu, J. K. Yim, J. Liang, Z. Shao, M. Qi, J. Zhong, Z. Luo, X. Yan, M. Zhang, X. Wang, *Sci. Robot.* **2019**, *4*, eaax1594.
- [219] J. Cao, L. Qin, J. Liu, Q. Ren, C. C. Foo, H. Wang, H. P. Lee, J. Zhu, *Extreme Mech. Lett.* **2018**, *21*, 9.
- [220] J. Bao, W. Chen, J. Xu, *IEEE Access* **2019**, *7*, 136792.
- [221] S. Kashima, F. Miyasaka, K. Hirata, *IEEE Trans. Magn.* **2012**, *48*, 1649.
- [222] J. Y. Kim, N. Mazzoleni, M. Bryant, in *Bioinspiration, Biomimetics, and Bioreplication XI*, Vol. 11586, International Society for Optics and Photonics, **2021**, p. 115860L.
- [223] C. T. Nguyen, H. Phung, H. Jung, U. Kim, T. D. Nguyen, J. Park, H. Moon, J. C. Koo, H. R. Choi, in *2015 IEEE ICRA*, IEEE, Piscataway, NJ **2015**, pp. 4484–4489.
- [224] A. Ming, K. Hashimoto, W. Zhao, M. Shimojo, in *2013 IEEE ICMA*, IEEE, Piscataway, NJ **2016**, pp. 219–224.
- [225] Q. Pei, R. Pelrine, S. Stanford, R. D. Kornbluh, M. S. Rosenthal, K. Meijer, R. J. Full, in *Smart Structures and Materials 2002: Industrial and Commercial Applications of Smart Structures Technologies*, Vol. 4698, International Society for Optics and Photonics, **2002**, pp. 246–253.
- [226] P. Polygerinos, Z. Wang, K. C. Galloway, R. J. Wood, C. J. Walsh, *Rob. Auton. Syst.* **2015**, *73*, 135.
- [227] S. Rosset, B. M. O'Brien, T. Gisby, D. Xu, H. R. Shea, I. A. Anderson, in *Smart Structures and Materials 2013: EAPAD*, Vol. 8687, International Society for Optics and Photonics, **2013**, p. 86872F.
- [228] G. Rizzello, F. Ferrante, D. Naso, S. Seelecke, *IEEE ASME Trans. Mechatron.* **2017**, *22*, 1705.
- [229] J. Cao, W. Liang, Q. Ren, U. Gupta, F. Chen, J. Zhu, in *2018 IEEE ICRA*, IEEE, Piscataway, NJ **2018**, pp. 1–9.
- [230] C.-C. Lan, C.-H. Fan, *Sens. Actuator A Phys.* **2010**, *163*, 323.
- [231] X. Tang, K. Li, W. Chen, D. Zhou, S. Liu, J. Zhao, Y. Liu, *Sens. Actuator A Phys.* **2019**, *285*, 319.
- [232] T. R. Lambert, A. Gurley, D. Beale, *Smart Mater. Struct.* **2017**, *26*, 035004.
- [233] A. Viloslada, A. Flores, D. Copaci, D. Blanco, L. Moreno, *Robot. Auton. Syst.* **2015**, *73*, 91.
- [234] J. Yin, T. Hellebrekers, C. Majidi, in *2020 3rd IEEE RoboSoft*, IEEE, Piscataway, NJ **2020**, pp. 661–667.
- [235] G. Rizzello, D. Naso, A. York, S. Seelecke, *IEEE Trans. Control Syst. Technol.* **2014**, *23*, 632.
- [236] B. Minorowicz, G. Leonetti, F. Stefanski, G. Binetti, D. Naso, *Smart Mater. Struct.* **2016**, *25*, 075005.
- [237] V. Cacucciolo, F. Renda, E. Poccia, C. Laschi, M. Cianchetti, *Smart Mater. Struct.* **2016**, *25*, 105020.
- [238] J. Kwon, S. J. Yoon, Y.-L. Park, *IEEE Trans. Robot.* **2020**, *36*, 743.
- [239] J. Wang, G. Chen, H. Wang, in *ASME 2019 IDETC-CIE*, Vol. 5B, ASME, **2019** <https://asmedigitalcollection.asme.org/IDETC-CIE/proceedings-pdf/IDETC-CIE2019/59247/V05BT07A003/6453802/v05bt07a003-detc2019-97174.pdf>.
- [240] J. Wang, G. Chen, Z. Zhang, J. Suo, H. Wang, *J. Mech. Robot.* **2021**, *1*.
- [241] A. Kapadia, I. D. Walker, in *2011 IEEE/RSJ IROS*, IEEE, Piscataway, NJ **2011**, pp. 1087–1092.
- [242] A. D. Kapadia, K. E. Fry, I. D. Walker, in *2014 IEEE/RSJ IROS*, IEEE, Piscataway, NJ **2014**, pp. 329–335.
- [243] U. K. Cheang, H. Kim, D. Milutinović, J. Choi, M. J. Kim, *J. Bionic Eng.* **2017**, *14*, 245.
- [244] A. Becker, Y. Ou, P. Kim, M. J. Kim, A. Julius, in *2013 IEEE/RSJ IROS*, IEEE, Piscataway, NJ **2013**, pp. 3317–3323.
- [245] K.-H. Lee, M. C. Leong, M. C. Chow, H.-C. Fu, W. Luk, K.-Y. Sze, C.-K. Yeung, K.-W. Kwok, in *2017 IEEE RCAR*, IEEE, Piscataway, NJ **2017**, pp. 11–16.
- [246] F. Xu, H. Wang, J. Wang, K. W. S. Au, W. Chen, *IEEE ASME Trans. Mechatron.* **2019**, *24*, 979.
- [247] J. A. Rogers, T. Someya, Y. Huang, *Science* **2010**, *327*, 1603.
- [248] M. L. Hammock, A. Chortos, B. C.-K. Tee, J. B.-H. Tok, Z. Bao, *Adv. Mater.* **2013**, *25*, 5997.
- [249] A. Chortos, J. Liu, Z. Bao, *Nat. Mater.* **2016**, *15*, 937.
- [250] M. Kaltenbrunner, T. Sekitani, J. Reeder, T. Yokota, K. Kuribara, T. Tokuhara, M. Drack, R. Schwödiauer, I. Graz, S. Bauer-Gogonea, S. Bauer, T. Someya, *Nature* **2013**, *499*, 458.
- [251] S. Wang, J. Xu, W. Wang, G.-J. N. Wang, R. Rastak, F. Molina-Lopez, J. W. Chung, S. Niu, V. R. Feig, J. Lopez, T. Lei, S.-K. Kwon, Y. Kim, A. M. Foudeh, A. Ehrlich, A. Gasperini, Y. Yun, B. Murmann, J. B.-H. Tok, Z. Bao, *Nature* **2018**, *555*, 83.
- [252] K.-J. Baeg, M. Caironi, Y.-Y. Noh, *Adv. Mater.* **2013**, *25*, 4210.
- [253] B. Kang, W. H. Lee, K. Cho, *ACS Appl. Mater. Interfaces* **2013**, *5*, 2302.
- [254] S. Jung, J. Kwon, S. Jung, in *Organic Flexible Electronics* **2021**, Elsevier, pp. 383–400.
- [255] J. W. Booth, J. C. Case, E. L. White, D. S. Shah, R. Kramer-Bottiglio, in *2018 IEEE RoboSoft*, IEEE, Piscataway, NJ **2018**, pp. 25–30.
- [256] R. Guo, H. Wang, M. Duan, W. Yu, X. Wang, J. Liu, *Smart Mater. Struct.* **2018**, *27*, 085022.
- [257] M. T. Tolley, R. F. Shepherd, B. Mosadegh, K. C. Galloway, M. Wehner, M. Karpelson, R. J. Wood, G. M. Whitesides, *Soft Robot.* **2014**, *1*, 213.
- [258] M. T. Tolley, R. F. Shepherd, M. Karpelson, N. W. Bartlett, K. C. Galloway, M. Wehner, R. Nunes, G. M. Whitesides, R. J. Wood, in *2014 IEEE/RSJ IROS*, IEEE, Piscataway, NJ **2014**, pp. 561–566.
- [259] G. Tortora, S. Caccavaro, P. Valdastri, A. Menciassi, P. Dario, in *2010 IEEE ICRA*, IEEE, Piscataway, NJ **2010**, pp. 1592–1597.
- [260] K. Zimmermann, V. Böhm, I. Zeidis, in *2011 IEEE/ASME AIM*, IEEE, Piscataway, NJ **2011**, pp. 730–735.
- [261] J.-E. Slotine, W. Li, *Applied Nonlinear Control*, Vol. 199, Prentice Hall, Englewood Cliffs, NJ **1991**.

- [262] M. Trumić, C. Della Santina, K. Jovanović, A. Fagiolini, in *2021 IEEE ACC*, IEEE, Piscataway, NJ **2021**, pp. 4991–4996.
- [263] D. Petković, A. S. Danesh, M. Dadkhah, N. Misaghian, S. Shamshirband, E. Zalnezhad, N. D. Pavlović, *Robot. Comput. Integrat. Manuf.* **2016**, 37, 170.
- [264] J. B. Rawlings, D. Q. Mayne, *Madison, Wisconsin* **2009**, 72.
- [265] D. Bruder, B. Gillespie, C. D. Remy, R. Vasudevan, *arXiv preprint arXiv:1902.02827*, **2019**.
- [266] J. Huang, Y. Cao, C. Xiong, H.-T. Zhang, *IEEE Trans. Autom. Sci. Eng.* **2018**, 16, 1071.
- [267] M. T. Gillespie, C. M. Best, E. C. Townsend, D. Wingate, M. D. Killpack, in *2018 IEEE RoboSoft*, IEEE, Piscataway, NJ **2018**, pp. 39–45.
- [268] M. C. Yip, D. B. Camarillo, *IEEE Trans. Robot.* **2014**, 30, 880.
- [269] T. George Thuruthel, E. Falotico, M. Manti, A. Pratesi, M. Cianchetti, C. Laschi, *Soft Robot.* **2017**, 4, 285.
- [270] M. H. Rosle, R. Kojima, K. Or, Z. Wang, S. Hirai, *IEEE Robot. Autom. Lett.* **2019**, 5, 159.
- [271] I. Van Meerbeek, C. De Sa, R. Shepherd, *Sci. Robot.* **2018**, 3, 24.
- [272] Y. Ansari, M. Manti, E. Falotico, M. Cianchetti, C. Laschi, *IEEE Robot. Autom. Lett.* **2017**, 3, 108.
- [273] M. Rolf, K. Neumann, J. F. Queißer, R. F. Reinhart, A. Nordmann, J. J. Steil, *Adv. Robot.* **2015**, 29, 847.
- [274] K.-H. Lee, D. K. Fu, M. C. Leong, M. Chow, H.-C. Fu, K. Althoefer, K. Y. Sze, C.-K. Yeung, K.-W. Kwok, *Soft Robot.* **2017**, 4, 324.
- [275] K. Chin, T. Hellebrekers, C. Majidi, *Adv. Intell. Syst.* **2020**, 2, 1900171.
- [276] T. G. Thuruthel, E. Falotico, M. Manti, C. Laschi, *IEEE Robot. Autom. Lett.* **2018**, 3, 1292.
- [277] M. Trumic, K. Jovanovic, A. Fagiolini, *Kernel-Based Nonlinear Adaptive Control of Stiffness and Position for Soft Robots Actuators*, Technical report.
- [278] C. Della Santina, M. Bianchi, G. Grioli, F. Angelini, M. Catalano, M. Garabini, A. Bicchi, *IEEE Robot. Autom. Mag.* **2017**, 24, 75.
- [279] F. Iida, R. Pfeifer, A. Seyfarth, in *50 Years of Artificial Intelligence*, Springer, **2007**, pp. 134–143.
- [280] C. Cheng, J. Cheng, W. Huang, *IEEE Access* **2019**, 7, 75073.
- [281] M. Giorelli, F. Renda, M. Calisti, A. Arienti, G. Ferri, C. Laschi, *Bioinspir. Biomim.* **2015**, 10, 035006.
- [282] M. E. Sayed, J. O. Roberts, R. M. McKenzie, S. Aracri, A. Buchoux, A. A. Stokes, *Soft Robot.* **2021**, 8, 319.
- [283] R. Suzuki, C. Zheng, Y. Kakehi, T. Yeh, E. Y.-L. Do, M. D. Gross, D. Leithinger, in *32nd ACM User Interface Software and Technology*, **2019**, pp. 493–505.
- [284] M. A. Robertson, J. Paik, *Sci. Robot.* **2017**, 2, 9.
- [285] R. L. Truby, J. A. Lewis, *Nature* **2016**, 540, 371.
- [286] E. Acome, S. Mitchell, T. Morrissey, M. Emmett, C. Benjamin, M. King, M. Radakovitz, C. Keplinger, *Science* **2018**, 359, 61.
- [287] X. Wang, S. K. Mitchell, E. H. Rumley, P. Rothemund, C. Keplinger, *Adv. Funct. Mater.* **2020**, 30, 1908821.
- [288] E. Leroy, R. Hinche, H. Shea, *Adv. Mater.* **2020**, 32, 2002564.
- [289] V. Cacucciolo, J. Shintake, Y. Kuwajima, S. Maeda, D. Floreano, H. Shea, *Nature* **2019**, 572, 516.
- [290] A. Miriyev, K. Stack, H. Lipson, *Nat. Commun.* **2017**, 8, 1.
- [291] D. J. Preston, P. Rothemund, H. J. Jiang, M. P. Nemitz, J. Rawson, Z. Suo, G. M. Whitesides, *Proc. Natl. Acad. Sci. U.S.A.* **2019**, 116, 7750.
- [292] G. Schwartz, B. C.-K. Tee, J. Mei, A. L. Appleton, D. H. Kim, H. Wang, Z. Bao, *Nat. Commun.* **2013**, 4, 1.
- [293] A. Marette, A. Poulin, N. Besse, S. Rosset, D. Briand, H. Shea, *Adv. Mater.* **2017**, 29, 1700880.
- [294] C. Kim, D. Espalin, M. Liang, H. Xin, A. Cuaron, I. Varela, E. Macdonald, R. B. Wicker, *IEEE Access* **2017**, 5, 25286.
- [295] D. R. Lesniak, K. L. Marshall, S. A. Wellnitz, B. A. Jenkins, Y. Baba, M. N. Rasband, G. J. Gerling, E. A. Lumpkin, *Elife* **2014**, 3, e01488.
- [296] W. W. Lee, Y. J. Tan, H. Yao, S. Li, H. H. See, M. Hon, K. A. Ng, B. Xiong, J. S. Ho, B. C. Tee, *Sci. Robot.* **2019**, 4, 32.
- [297] B. Xia, J. Fu, H. Zhu, Z. Song, Y. Jiang, H. Lipson, *arXiv preprint arXiv:2011.06749* **2020**.
- [298] K. Melo, M. Garabini, G. Grioli, M. Catalano, L. Malagia, A. Bicchi, in *Robot Makers-Workshop in conjunction with 2014 Robotics Science and Systems Conf.*, **2014**, pp. 1–5.
- [299] Y. Ohmura, Y. Kuriyoshi, A. Nagakubo, in *2006 IEEE ICRA*, IEEE, Piscataway, NJ **2006**, pp. 1348–1353.
- [300] W. W. Lee, S. L. Kukreja, N. V. Thakor, in *2015 IEEE BioCAS*, IEEE, Piscataway, NJ **2015**, pp. 1–4.
- [301] B. Aksoy, H. Shea, *Adv. Funct. Mater.* **2020**, 30, 2001597.
- [302] K. Suzumori, A. Wada, S. Wakimoto, *Sens. Actuator A Phys.* **2013**, 201, 148.
- [303] K. Sim, F. Ershad, Y. Zhang, P. Yang, H. Shim, Z. Rao, Y. Lu, A. Thukral, A. Elgalad, Y. Xi, B. Tian, D. A. Taylor, C. Yu, *Nat. Electron.* **2020**, 3, 775.
- [304] K. Ikuta, H. Ichikawa, K. Suzuki, D. Yajima, in *Proc. 2006 IEEE Int. Conf. on Robotics and Automation, 2006. ICRA 2006*, IEEE, Piscataway, NJ **2006**, pp. 4161–4166.
- [305] M. M. Ali, K. Takahata, *J. Micromech. Microeng.* **2011**, 21, 075005.
- [306] X. Yu, Z. Xie, Y. Yu, J. Lee, A. Vazquez-Guardado, H. Luan, J. Ruban, X. Ning, A. Akhtar, D. Li, B. Ji, Y. Liu, R. Sun, J. Cao, Q. Huo, Y. Zhong, C. Lee, S. Kim, P. Gutruf, C. Zhang, Y. Xue, Q. Guo, A. Chempakasseril, P. Tian, W. Lu, J. Jeong, Y. Yu, J. Cornman, C. Tan, B. Kim, K. Lee, X. Feng, Y. Huang, *Nature* **2019**, 575, 473.
- [307] E. Diller, S. Floyd, C. Pawashe, M. Sitti, *IEEE Trans. Robot.* **2011**, 28, 172.
- [308] U. Kei Cheang, K. Lee, A. A. Julius, M. J. Kim, *Appl. Phys. Lett.* **2014**, 105, 083705.
- [309] A. W. Mahoney, N. D. Nelson, K. E. Peyer, B. J. Nelson, J. J. Abbott, *Appl. Phys. Lett.* **2014**, 104, 144101.
- [310] D. Wong, E. B. Steager, V. Kumar, *IEEE Robot. Autom. Lett.* **2016**, 1, 554.
- [311] S. R. Mishra, *Selective Actuation of Polymer Nanocomposites by Controlling Properties of Magnetic and Plasmonic Nanoparticles for Soft Robotics Applications*, North Carolina State University, **2017**.
- [312] D. R. Frutiger, Ph.D. thesis, ETH, **2010**.
- [313] T. Bretl, *Robot.: Sci. Syst.* **2008**, 209.
- [314] S. Huang, Y. Huang, Q. Li, *Small Struct.* **2021**, 2, 2100038.
- [315] J. Xu, N. Zhao, B. Qin, M. Qu, X. Wang, B. Ridi, C. Li, Y. Gao, *ACS Appl. Mater. Interfaces* **2021**, 13, 44833.
- [316] Y. Huang, H. K. Bisoyi, S. Huang, M. Wang, X.-M. Chen, Z. Liu, H. Yang, Q. Li, *Angew. Chem., Int. Ed.* **2021**, 60, 11247.
- [317] B. Zuo, M. Wang, B.-P. Lin, H. Yang, *Nat. Commun.* **2019**, 10, 1.
- [318] R. R. Kohlmeyer, J. Chen, *Angew. Chem., Int. Ed.* **2013**, 125, 9404.
- [319] T.-Y. Huang, M. S. Sakar, A. Mao, A. J. Petruska, F. Qiu, X.-B. Chen, S. Kennedy, D. Mooney, B. J. Nelson, *Adv. Mater.* **2015**, 27, 6644.
- [320] S. Kim, F. Qiu, S. Kim, A. Ghanbari, C. Moon, L. Zhang, B. J. Nelson, H. Choi, *Adv. Mater.* **2013**, 25, 5863.
- [321] M. Medina-Sánchez, L. Schwarz, A. K. Meyer, F. Hebenstreit, O. G. Schmidt, *Nano Lett.* **2016**, 16, 555.
- [322] J. Kim, S. E. Chung, S.-E. Choi, H. Lee, J. Kim, S. Kwon, *Nat. Mater.* **2011**, 10, 747.
- [323] D. Kokkinis, M. Schaffner, A. R. Studart, *Nat. Commun.* **2015**, 6, 1.
- [324] R. Dreyfus, J. Baudry, M. L. Roper, M. Fermigier, H. A. Stone, J. Bibette, *Nature* **2005**, 437, 862.
- [325] J. Zhang, O. Onaizah, K. Middleton, L. You, E. Diller, *IEEE Robot. Autom. Lett.* **2017**, 2, 835.
- [326] Z. Z. Bandic, R. H. Victora, *Proc. IEEE* **2008**, 96, 1749.

- [327] E. Diller, J. Zhuang, G. Zhan Lum, M. R. Edwards, M. Sitti, *Appl. Phys. Lett.* **2014**, *104*, 174101.
- [328] G. Z. Lum, Z. Ye, X. Dong, H. Marvi, O. Erin, W. Hu, M. Sitti, *Proc. Natl. Acad. Sci. U.S.A.* **2016**, *113*, E6007.
- [329] W. Hu, G. Z. Lum, M. Mastrangeli, M. Sitti, *Nature* **2018**, *554*, 81.
- [330] Y.-F. Zhang, N. Zhang, H. Hingorani, N. Ding, D. Wang, C. Yuan, B. Zhang, G. Gu, Q. Ge, *Adv. Funct. Mater.* **2019**, *29*, 1806698.
- [331] A. K. Mishra, W. Pan, E. P. Giannelis, R. F. Shepherd, T. J. Wallin, *Nat. Protoc.* **2021**, *16*, 2068.
- [332] C. Paul, *Rob. Auton. Syst.* **2006**, *54*, 619.
- [333] C. Laschi, B. Mazzolai, *IEEE Robot. Autom. Mag.* **2016**, *23*, 107.
- [334] C. Stefanini, S. Orofino, L. Manfredi, S. Mintchev, S. Marrazza, T. Assaf, L. Capantini, E. Sinibaldi, S. Grillner, P. Wallén, P. Dario, *Bioinspir. Biomim.* **2012**, *7*, 025001.
- [335] M. Ziegler, F. Iida, R. Pfeifer, in *CLAWAR 2006*, **2006**.
- [336] Y. Gutfreund, T. Flash, G. Fiorito, B. Hochner, *J. Neurosci.* **1998**, *18*, 5976.
- [337] B. Hochner, *Curr. Biol.* **2012**, *22*, R887.
- [338] C. L. Huffard, F. Boneka, R. J. Full, *Science* **2005**, *307*, 1927.
- [339] M. Calisti, M. Giorelli, G. Levy, B. Mazzolai, B. Hochner, C. Laschi, P. Dario, *Bioinspir. Biomim.* **2011**, *6*, 036002.
- [340] M. Cianchetti, M. Calisti, L. Margheri, M. Kuba, C. Laschi, *Bioinspir. Biomim.* **2015**, *10*, 035003.
- [341] C. Laschi, M. Cianchetti, B. Mazzolai, L. Margheri, M. Follador, P. Dario, *Adv. Robot.* **2012**, *26*, 709.
- [342] K. Kumar, J. Liu, C. Christianson, M. Ali, M. T. Tolley, J. Aizenberg, D. E. Ingber, J. C. Weaver, K. Bertoldi, *Soft Robot.* **2017**, *4*, 317.
- [343] B. Shih, D. Shah, J. Li, T. G. Thuruthel, Y.-L. Park, F. Iida, Z. Bao, R. Kramer-Bottiglio, M. T. Tolley, *Sci. Robot.* **2020**, *5*, 41.
- [344] S. S. Robinson, K. W. O'Brien, H. Zhao, B. N. Peele, C. M. Larson, B. C. Mac Murray, I. M. Van Meerbeek, S. N. Dunham, R. F. Shepherd, *Extreme Mech. Lett.* **2015**, *5*, 47.
- [345] R. L. Truby, M. Wehner, A. K. Grosskopf, D. M. Vogt, S. G. Uzel, R. J. Wood, J. A. Lewis, *Adv. Mater.* **2018**, *30*, 1706383.
- [346] Y. Kim, A. Chortos, W. Xu, Y. Liu, J. Y. Oh, D. Son, J. Kang, A. M. Foudeh, C. Zhu, Y. Lee, S. Niu, J. Liu, R. Pfaffner, Z. Bao, T.-W. Lee, *Science* **2018**, *360*, 998.
- [347] M. Wang, Y. Luo, T. Wang, C. Wan, L. Pan, S. Pan, K. He, A. Neo, X. Chen, *Adv. Mater.* **2021**, *33*, 2003014.
- [348] N. Cheney, R. MacCurdy, J. Clune, H. Lipson, *ACM SIGEVolution* **2014**, *7*, 11.
- [349] N. Liu, L. Q. Zhu, P. Feng, C. J. Wan, Y. H. Liu, Y. Shi, Q. Wan, *Sci. Rep.* **2015**, *5*, 18082.
- [350] J. Till, V. Aloj, C. Rucker, *Int. J. Rob. Res.* **2019**, *38*, 723.
- [351] B. Zhang, Y. Fan, P. Yang, T. Cao, H. Liao, *Soft Robot.* **2019**, *6*, 399.
- [352] J. Till, C. E. Bryson, S. Chung, A. Orekhov, D. C. Rucker, in *2015 IEEE ICRA*, IEEE, Piscataway, NJ **2015**, pp. 5067–5074.
- [353] Q. He, Z. Wang, Y. Wang, A. Minor, M. T. Tolley, S. Cai, *Sci. Adv.* **2019**, *5*, 5746.
- [354] M. Matysek, P. Lotz, H. F. Schlaak, in *EAPAD 2009*, Vol. 7287, International Society for Optics and Photonics, **2009**, p. 72871D.
- [355] N. Besse, S. Rosset, J. J. Zarate, H. Shea, *Adv. Mater. Technol.* **2017**, *2*, 1700102.



**Jue Wang** received his B.S. degree from Dalian University of Technology, Dalian, China, in 2017 and M.S. degree from Shanghai Jiao Tong University, Shanghai, China, in 2020. He is currently a Ph.D. candidate in the College of Engineering, Purdue University. His research interests include soft robotics, magnetic control, and 3D printing.



**Alex Chortos** completed his B.A.Sc in nanotechnology engineering at the University of Waterloo in 2011 and Ph.D. at Stanford University in 2017 under the guidance of Zhenan Bao. After finishing his postdoctoral fellow at Harvard University in 2020, he is currently an assistant professor at Purdue University. His research background includes bio-inspired tactile sensors, stretchable circuits, and soft actuators. His lab leverages the capabilities of 3D printing combined with materials design to pursue new device strategies for bio-integrated electronics.